


RESEARCH PAPER

Glycogen synthase kinase-3 inhibition rescues sex-dependent contextual fear memory deficit in human immunodeficiency virus-1 transgenic mice

Shamsudheen Moidunny¹  | Michael A. Benneyworth² | David J. Titus^{2,3} |
 Eleonore Beurel⁴ | Udghatri Kolli¹ | Joyce Meints² | Richa Jalodia¹ |
 Sundaram Ramakrishnan¹ | Coleen M. Atkins³ | Sabita Roy¹

¹Department of Surgery, University of Miami Miller School of Medicine, Miami, FL, USA

²Department of Neuroscience, University of Minnesota, Minneapolis, MN, USA

³The Miami Project to Cure Paralysis, Department of Neurological Surgery, University of Miami Miller School of Medicine, Miami, FL, USA

⁴Department of Psychiatry and Behavioral Sciences, Department of Biochemistry and Molecular Biology, University of Miami Miller School of Medicine, Miami, FL, USA

Correspondence

Sabita Roy, Department of Surgery, University of Miami Miller School of Medicine, 1501 NW 10th Ave, BRB 514, Miami, FL 33136, USA.
 Email: sabita.roy@miami.edu

Shamsudheen Moidunny, Department of Surgery, University of Miami Miller School of Medicine, 1501 NW 10th Ave, BRB 509, Miami, FL 33136, USA.
 Email: sxm1464@med.miami.edu

Funding information

National Institutes of Health, Grant/Award Numbers: R01 DA050542, R01 DA047089, R01 DA043252 and R01 DA044582; Miami Center for AIDS Research (CFAR), Grant/Award Number: P30AI073961

Background and Purpose: A significant number of HIV-1 patients on antiretroviral therapy develop HIV-associated neurocognitive disorders (HAND). Evidence indicate that biological sex may regulate HAND pathogenesis, but the mechanisms remain unknown. We investigated synaptic mechanisms associated with sex differences in HAND, using the HIV-1-transgenic 26 (Tg26) mouse model.

Experimental Approach: Contextual- and cue-dependent memories of male and female Tg26 mice and littermate wild type mice were assessed in a fear conditioning paradigm. Hippocampal electrophysiology, immunohistochemistry, western blot, qRT-PCR and ELISA techniques were used to investigate cellular, synaptic and molecular impairments.

Key Results: Cue-dependent memory was unaltered in male and female Tg26 mice, when compared to wild type mice. Male, but not female, Tg26 mice showed deficits in contextual fear memory. Consistently, only male Tg26 mice showed depressed hippocampal basal synaptic transmission and impaired LTP induction in area CA1. These deficits in male Tg26 mice were independent of hippocampal neuronal loss and microglial activation but were associated with increased HIV-1 long terminal repeat mRNA expression, reduced hippocampal synapsin-1 protein, reduced BDNF mRNA and protein, reduced AMPA glutamate receptor (GluA1) phosphorylation levels and increased glycogen synthase kinase 3 (GSK3) activity. Importantly, selective GSK3 inhibition using 4-benzyl-2-methyl-1,2,4-thiadiazolidine-3,5-dione increased levels of synapsin-1, BDNF and phosphorylated-GluA1 proteins, restored hippocampal basal

Abbreviations: BDNF, brain derived neurotrophic factor; CA1, cornu ammonis-1; CA3, cornu ammonis-3; fEPSP, field excitatory post synaptic potential; Gp120, glycoprotein 120; GSK3, glycogen synthase kinase 3; HAND, HIV-associated neurocognitive disorders; H&E, haematoxylin and eosin; HIV-1, human immunodeficiency virus-1; LTR, long terminal repeat; Iba-1, ionized calcium binding adaptor molecule 1; LTP, long-term potentiation; Ngf, nerve growth factor; Ntf-3, neurotrophin-3; Ntf-4/5, neurotrophin-4/5; qRT-PCR, quantitative reverse transcriptase-PCR; RIPA, radioimmunoprecipitation assay; Rpl32, ribosomal protein L32; Rps18, ribosomal protein s18; TDZD-8, 4-benzyl-2-methyl-1,2,4-thiadiazolidine-3,5-dione; Tg26, HIV-1-transgenic 26; WT, wild type.

Michael A. Benneyworth, David J. Titus and Eleonore Beurel contributed equally to this study.

synaptic transmission and LTP, and improved contextual fear memory in male Tg26 mice.

Conclusion and Implications: Sex-dependent impairments in contextual fear memory and synaptic plasticity in Tg26 mice are associated with increased GSK3 activity. This implicates GSK3 inhibition as a potential therapeutic strategy to improve cognition in HIV-1 patients.

KEYWORDS

BDNF, GSK3, HAND, hippocampus, sex difference, synapsin-1, Tg26

1 | INTRODUCTION

HIV-associated neurocognitive disorders (HAND), especially the milder forms, continue to afflict over 50% of HIV patients receiving antiretroviral therapies (ART), causing significant health burden in affected individuals (Saylor et al., 2016). The severity of HAND, given its naturally progressive and irreversible course, is rising as the majority of people living with HIV-1 are over 50 years of age (Goodkin et al., 2017; Valcour et al., 2004). Recent evidence indicate that the development of HAND may be differentially regulated in men and women (Faílde-Garrido, Alvarez, & Simón-López, 2008; Fogel et al., 2017; Keutmann et al., 2017; Robertson et al., 2014; Wisniewski et al., 2005). For example, HIV-infected men compared to women showed poorer performance in verbal memory tests, whereas cocaine-dependent HIV-infected women showed poorer episodic memory (Fogel et al., 2017; Keutmann et al., 2017; Wisniewski et al., 2005). While limited studies have also indicated sex differences in animal models of HAND, the underlying mechanisms remain largely unknown (Hahn et al., 2015; McLaurin, Booze, & Mactutus, 2018; McLaurin, Booze, Mactutus, & Fairchild, 2017; Putatunda et al., 2019). Thus, understanding the role of biological sex in HAND is important as it may unveil pathways that can be targeted to optimize treatments in HIV patients.

In this study, we investigated mechanisms underlying sex differences in HAND, using the HIV-1 transgenic (Tg26) mouse model (Dickie et al., 1991). Tg26 mice constitutively express 7 of the 9 HIV-1 genes, which allows investigation of long-term effects of latent HIV-1 infection and HIV-1 proviral proteins in HAND pathogenesis. A recent study found HIV-1 transcripts in the hippocampal dentate gyrus of Tg26 mice, which consistently showed reduced hippocampal neurogenesis and dendritic abnormalities in the newborn mature granule neurons (Putatunda et al., 2018), suggesting a potential direct effect of HIV-1 transcripts on the hippocampal function. However, the onset of cognitive impairments and the underlying synaptic mechanisms in Tg26 mice have not been investigated thus far. We therefore conducted a comprehensive behavioural, electrophysiological and molecular analysis of hippocampal-dependent learning and memory in young adult male and female Tg26 mice to identify potential therapeutic targets, especially since memory deficits pertaining to hippocampal

What is already known

- HIV-1 patients on antiretroviral therapy continue to develop HIV-associated neurocognitive disorders (HAND).
- Sex differences in HAND have been reported, but the mechanisms remain unknown.

What does this study adds

- Male, but not female, HIV-1-transgenic mice show deficits in contextual fear memory and hippocampal synaptic plasticity.
- GSK 3 inhibition rescues synaptic plasticity deficits and improves contextual fear memory in HIV-1-transgenic mice.

What is the clinical significance

- GSK 3 inhibition may rescue hippocampal-dependent learning and memory deficits in HIV-1 patients.

dysfunction are commonly observed in HIV patients on antiretroviral therapy (Goodkin et al., 2017).

Emerging evidence implicate inhibitors of **glycogen synthase kinase 3 (GSK3)**, a serine/threonine kinase, as promising rescuers of cognitive impairments associated with Alzheimer's disease, Parkinson's disease, Fragile X syndrome and traumatic brain injury (Franklin et al., 2014; King et al., 2014; Martinez, Alonso, Castro, Perez, & Moreno, 2002). GSK3 was first described as the kinase that phosphorylates glycogen synthase but has been identified to phosphorylate over 50 substrates, implicating GSK3 in a variety of cellular functions (Woodgett, 1990). Interestingly, GSK3 inhibition reduces HIV-1 induced neurotoxicity both in vitro and in vivo and inhibits gp120-induced glial activation in vivo (Everall et al., 2002; Maggirwar,

Tong, Ramirez, Gelbard, & Dewhurst, 1999; Masvekar, El-Hage, Hauser, & Knapp, 2015). However, it remains unclear whether GSK3 inhibition would have therapeutic benefits in HAND. In this study, we further investigated the effects of GSK3 inhibition on hippocampal synaptic transmission and memory in Tg26 mice.

2 | METHODS

2.1 | Animals

All animal care and experimental procedures were in strict accordance with the United States National Institutes of Health's guidelines for Care and Use of Laboratory Animals and were approved by the Institutional Animal Care and Use Committee of the University of Minnesota (Protocols 1203A11091 and 1404A31457) and the University of Miami (Protocols 17-103 and 20-100-LF). Animal studies are reported in compliance with the ARRIVE guidelines (Percie du Sert et al., 2020) and with the recommendations made by the *British Journal of Pharmacology* (Lilley et al., 2020). In this study, we utilized 4–5 months old adult male and female NL4-3 $\Delta gag/pol$ transgenic Tg26 mice of C57BL/6 background (Putatunda et al., 2018) and the age-matched littermate wild type (WT) mice as controls. Body weights were approximately 37 g for male WT, 29 g for male Tg26, 26 g for female WT and 22 g for female Tg26 mice. Tg26 mouse expresses a 7.4 kb transgene containing the genetic sequence for the HIV-1 *tat*, *env*, *rev*, *nef*, *vif*, *vpr* and *vpu* genes, which are transcriptionally regulated by the long terminal repeat (LTR) promoter (Dickie et al., 1991). Tg26 mouse breeders were obtained from Dr. Roy Lee Sutliff's Laboratory at Emory University School of Medicine (Atlanta, GA) and the colony was expanded and maintained under specific pathogen free conditions. All litters produced were genotyped from

tail biopsies collected at the time of weaning (3 weeks of age). The littermate WT and Tg26 mice were co-housed in groups of three to five animals in standard makrolon cages containing rich bedding made of dried wood chips. They were maintained on a 12-h light/dark cycle and had free access to food and water under clean, temperature-controlled conditions. The Tg26 mice in C57BL/6 background have longer life expectancies. However, approximately 10% of Tg26 mice spontaneously develop skin lesions with characteristics of B cell lymphoma and these animals were excluded from our studies. In addition, female Tg26 mice displayed infanticidal behaviours which resulted in uneven sample sizes in some of the experiments described here. At the end of experiments, all animals were deeply anaesthetized with 4% isoflurane and killed by decapitation of the head. The different brain regions (hippocampus and amygdala) were quickly dissected and snap frozen in liquid nitrogen.

2.2 | Detection of proviral DNA in Tg26 mouse hippocampus

Hippocampal tissues were lysed overnight at 55°C in Cell Lysis Solution (Qiagen, cat: 158906) supplemented with Proteinase K (0.2 mg·ml⁻¹; Lamda Biotech, cat: DB0451). Total genomic DNA was extracted using the conventional phenol-chloroform method, followed by ethanol precipitation. The quality of DNA was assessed with a NanoDrop Lite Spectrophotometer (Thermo Scientific). PCR reactions were set up for HIV-1 LTR, *tat*, *nef* and 18 s primers (see Table 1) using the REExtract-N-Amp PCR ReadyMix (Sigma-Aldrich, cat: R4775). Amplified PCR products were run through a 1.5% agarose gel. Gels were imaged using a ChemiDoc MP Imaging System (Bio-Rad Laboratories; RRID: SCR_008426). The sizes of DNA bands on the gel were verified by comparison with 100 bp DNA Ladder

TABLE 1 List of primers and TaqMan assay probes used for PCRs (qRT-PCR and genomic DNA PCR)

Gene	Forward primer (5'-3')	Backward primer (5'-3')
Rpl32	GCTGGAGGTGCTGCTGATGT	ACTCTGATGGCCAGCTGTGC
Bdnf	GGAATTCACCATGGAGCCAGTAGATCCT	GCCACAAGCAGGAATGAGAA
Tnf- α	GACTCTGGAGAGCGTGAAT	GCCACAAGCAGGAATGAGAA
Il6	GACGTGGAAGTGGCAGAAGA	TCCACGATTTCCAGAGAAC
Cox-2	CCGGAGAGGAGACTTCACAG	CCCAAAGATAGCATCTGGA
HIV-1 LTR	CTCCCTGAAGCCGTACACAT	CTGCTAGAGATTTCCACACTG
HIV-1 <i>nef</i>	GGTCTCTCTGGTTAGACCAGAT	TCAGCAGTTCTTGAAGTACTC
HIV-1 <i>tat</i>	ATGGGTGCAAGTGGTCAA	CGGGATCCCTATTCCCTTCGGGCCTGT
18s	GGAATTCACCATGGAGCCAGTAGATCCT	ACGCTGAGCCAGTCAGTGTA
Gapdh	CTTAGAGGGACAAGTGCGG	GCCTGCTTCAACACCTTCTTGATG
Gene	Company	TaqMan Assay Probe ID
Ngf	Applied Biosystems	Mm00443039_m1
Ntf-3	Applied Biosystems	Mm01182924_m1
Ntf-4/5	Applied Biosystems	Mm01701591_m1
Rps18	Applied Biosystems	Mm02601777_g1

(Invitrogen, cat: 15628-019). This protocol was used for genotyping Tg26 mice from tail biopsies, using the *nef* primers (see Table 1).

2.3 | GSK3 inhibition

GSK3 inhibition was achieved using **4-benzyl-2-methyl-1,2,4-thiadiazolidine-3,5-dione (TDZD-8)**, a highly selective non-ATP competitive **GSK3 β** inhibitor (Franklin et al., 2014; Martinez, Alonso, Castro, Perez, & Moreno, 2002; Xie et al., 2016). Briefly, mice were weighed and intraperitoneally treated with TDZD-8 (5 mg·kg⁻¹; prepared in saline containing 5% Tween-80 and 5% DMSO) for 24 h. Control animals were treated with an equivalent volume of 0.9% saline (containing 5% Tween-80 and 5% DMSO) for 24 h. The dosage and method of drug treatment used in this study were determined based on a previously published work (Franklin et al., 2014). We confirmed the efficacy of TDZD-8 treatment (5 mg·kg⁻¹ for 24 h) to inhibit hippocampal GSK3 activity in WT and Tg26 mice, by measuring the inhibitory phosphorylation (at Ser9) of GSK3 β protein using western blot technique (see Section 3.4). The inability to detect phosphorylated **GSK3 α** proteins in hippocampal tissue lysates by western blotting precluded any analysis of the effect of TDZD-8 treatment on GSK3 α activity. TDZD-8 treatment for 24 h did not alter body weights of male WT or Tg26 mice.

2.4 | Behavioural pre-screening

WT and Tg26 mice of both sexes were assessed for sensory and motor impairments through a battery of observational tasks in a modified SHIRPA (SmithKline Beecham, Harwell, Imperial College, Royal London Hospital Phenotype Assessment) screen (Rogers et al., 1997). Briefly, animals were weighed and observed for spontaneous activity, grooming and general appearance, righting reflex, bite irritability, pupil reflex, visual placement reflex, gross grip reflex and wire manoeuvre performance. Spontaneous activity was assessed for any unusual behaviours (stereotypies and gate issues) and was scored as follows: 0 = none, resting; 1 = casual scratch, groom, slow movement; 2 = vigorous scratch, groom, moderate movement; 3 = vigorous, rapid/dart movement; 4 = extremely vigorous, rapid/dart movement. For measuring righting reflex, the mouse was held by the tail and flicked backwards through the air such that it performs a backward somersault when released and the landing position was observed (score 0 = fails to right when placed on back; 1 = lands on back; 2 = lands on side; 3 = no impairment). For measuring bite irritability, the mouse was prodded with cotton swab and the response was recorded (score 0 = no response; 1 = slight attack; 2 = moderate attack; 3 = marked attack). For assessing pupil reflex, a small pen light was directed at the eye to cause pupil constriction. Size of constricted pupil was noted as pinpoint (0.5 mm), 1, 2 or 3 mm. For visual reflex measure, extension of forelimbs was noted when the mouse was lowered by base of the tail from a height of

approximately 15 cm above wire grid (score 0 = none; 1 = upon nose contact; 2 = upon vibrissae contact; 3 = before vibrissae contact (18 mm); 4 = early vigorous extension (25 mm)). For measuring grip strength, the mouse was lowered and allowed to grip the cage grid, following which a gentle horizontal backwards pull was applied (score 0 = none; 1 = slight grip, semi-effective; 2 = moderate grip, effective; 3 = active grip, effective; 4 = unusually effective). For wire manoeuvre test, the mouse was held above the wire by tail suspension and lowered to allow the forelimbs to grip the horizontal wire. The mouse was held in extension and rotated around to the horizontal and released (score 0 = falls immediately; 1 = unable to lift hindlegs, falls within seconds; 2 = unable to grasp with hindlegs; 3 = difficulty to grasp with hindlegs; 4 = active grip with hindlegs). Body temperature of the mouse was measured by gently inserting a probe covered with Vaseline into the rectum to up to 2 cm depth.

2.5 | Fear conditioning

Contextual and cued fear memory were assessed using a fear conditioning paradigm (Martin-Fernandez et al., 2017). Briefly, mice were conditioned in sound-attenuated chambers where a discrete auditory (80 dB white noise) and visual cue (dim house light) was presented for 15 s and co-terminated with a foot shock (0.7 mA for 1 s). Freezing responses during the inter-trial interval periods (45 s each) between the five cue-shock pairings were analysed using the Video Freeze software (Med Associate Inc.); 24 h later, mice were returned to the test chambers for a 2 min context memory test. All elements (visual, tactile and olfactory) remained consistent with conditioning. Two hours after the context test, contextual elements were changed (wall and floor inserts added, olfactory cues changed from 33% Simple Green solution to 1% vanilla) and mice were reintroduced to the test chambers to measure their baseline freezing (non-specific fear) for 2 min. This was followed by a 2 min cued-freezing test, where the auditory and visual cues were returned. Fear responses of mouse during conditioning and test sessions are expressed as % time the animal spends freezing, in order to reduce unwanted sources of variation. To determine the effect of fear conditioning on hippocampal GluA1 protein phosphorylation, mice were killed 30 min after the conditioning session. For fear conditioning experiments involving TDZD-8, drug was administered 30 min prior to the start of the conditioning session.

2.6 | Electrophysiology

Field excitatory post synaptic potentials (fEPSPs) were recorded from hippocampal CA1 stratum radiatum in response to Schaffer collateral stimulation, as previously described (Titus et al., 2016). Briefly, mice were decapitated under anaesthesia with 4% isoflurane, for 1–2 min. The hippocampus was quickly isolated and

transversely sliced at 400 μm thickness in sucrose-based artificial CSF (aCSF) containing the following (in mM): 110 sucrose, 60 NaCl, 3 KCl, 1.25 NaH_2PO_4 , 28 NaHCO_3 , 7 MgCl_2 , 0.5 CaCl_2 , 5 D-glucose and equilibrated with 95% O_2 and 5% CO_2 at 4°C. The slices were transferred to a submerged recording chamber following 20 min in 50:50 sucrose-based aCSF and standard aCSF (in mM: 125 NaCl, 2.5 KCl, 1.25 NaH_2PO_4 , 25 NaHCO_3 , 10 D-glucose, 2 CaCl_2 , 1 MgCl_2 , saturated with 95% O_2 /5% CO_2) and then in standard aCSF for 1 h at room temperature recovery. The electrophysiological responses were low pass filtered at 2 kHz and recorded with Multiclamp 700B. The signals were digitized at 20 kHz with a Digidata 1440A interface and pClamp 10.4 software (Molecular Devices; RRID: SCR_011323). Input-output (IO) curves were generated by measuring the slope of fEPSPs in response to increasing current intensities (20 to 200 μA). Baseline responses were recorded at 40–50% of the maximum fEPSP at 0.033 Hz for 20 min before induction of LTP with a high-frequency stimulation of 100 pulses delivered at 100 Hz at a t-test stimulation intensity.

2.7 | Immunohistochemistry

Immunostaining of paraffin-embedded sagittal brain sections was performed as previously described (Divani et al., 2015). Briefly, mice were perfused intracardially with saline (0.9% w/v) followed by 4% paraformaldehyde. Brains were dissected and fixed in 4% paraformaldehyde. Sagittal sections of paraffin-embedded mouse brains were cut at 10 μm thickness and transferred to Superfrost Plus Microscopic slides (Fisher Scientific, cat: 12-550-15). Dried tissue slides were heated at 57°C for 30 min, de-paraffinized in xylene and rehydrated through a series of graded ethanol. Antigen-retrieval was performed using Reveal Decloaker (Biocare Medical, cat: RV1000M) in a steamer for 30 min. Immunostaining of the tissue sections was performed manually. Briefly, tissue sections were incubated for about 13 min with Background Sniper (Biocare Medical, cat: BS966 MM) to block the endogenous peroxidase activity, followed by overnight incubation at 4°C with appropriate primary antibody (diluted in a solution of 5% Background Sniper and 1% Tris-buffered saline with Tween 20). See Table 2 for antibody details and dilutions used. Following primary

TABLE 2 List of primary and secondary antibodies used for western blot (WB) and immunohistochemistry (IHC)

Antibody	Host	Company	Catalogue No	RRID	Dilutions used for WB or IHC
Anti-phospho Ser831 GluA1	Rabbit	Millipore	04-823	AB_1977218	1:1000 (WB)
Anti-Synaptophysin	Mouse	Millipore	MAB5258	AB_2313839	1:1000 (WB)
Anti-GSK3 α + β	Mouse	Millipore	05-412	AB_309720	1:2000 (WB)
Anti-GSK3 β	Mouse	Abcam	ab93926	AB_10563643	1:2000 (WB)
Anti-GluA2/3	Rabbit	Abcam	ab52896	AB_880229	1:1000 (WB)
Anti-phospho Ser418 PSD95	Rabbit	Abcam	ab16493	AB_777514	1:1000 (WB)
Anti-SNAP25	Rabbit	Abcam	ab5666	AB_305033	1:500 (WB)
Anti-Syntaxin-1a	Rabbit	Abcam	ab41453	AB_956343	1:1000 (WB)
Anti-pan Cadherin	Mouse	Abcam	ab6528	AB_305544	1:1000 (WB)
Anti-NMDA receptor 1	Rabbit	ThermoFisher Scientific	PA3-102	AB_2112003	1:500 (WB)
Anti-NMDA receptor 2A	Rabbit	Cell Signaling Technology	4205	AB_2112295	1:1000 (WB)
Anti-NMDA receptor 2B	Rabbit	Cell Signaling Technology	4207	AB_1264223	1:1000 (WB)
Anti-Synapsin-1	Rabbit	Cell Signaling Technology	5297	AB_2616578	1:1000 (WB)
Anti-Synaptobrevin	Rabbit	Cell Signaling Technology	13508	AB_2798240	1:1000 (WB)
Anti-p75 NTR	Rabbit	Cell Signaling Technology	8238	AB_10839265	1:2000 (WB)
Anti-phospho Ser9 GSK3 β	Rabbit	Cell Signaling Technology	9336	AB_331405	1:1000 (WB)
Anti- β -actin	Mouse	Cell Signaling Technology	3700	AB_2242334	1:2000 (WB)
Anti- β -actin	Rabbit	Cell Signaling Technology	4967	AB_330288	1:1000 (WB)
Anti-GAPDH	Rabbit	Cell Signaling Technology	2118	AB_561053	1:3000 (WB)
Anti-Synaptotagmin 2	Goat	Santa Cruz Biotech	sc12465	AB_2199474	1:500 (WB)
Anti-Gephyrin	Rabbit	Santa Cruz Biotech	sc14003	AB_640963	1:200 (WB)
Anti-TrkB	Goat	R&D Systems	AF1494	AB_2155264	1:200 (WB)
Anti-Goat IgG (H + L) IRDye 800CW	Donkey	LI-COR Biosciences	925-32214	AB_2687553	1:8000 (WB)
Anti-Mouse IgG (H + L) IRDye 680RD	Donkey	LI-COR Biosciences	926-68072	AB_10953628	1:8000 (WB)
Anti-Rabbit IgG (H + L) IRDye 800CW	Donkey	LI-COR Biosciences	925-32213	AB_2715510	1:8000 (WB)
Anti-Iba-1	Goat	Abcam	ab5076	AB_2224402	1:1000 (WB)
Anti-Iba-1	Rabbit	Wako Chemical	019-19741	AB_839504	1:500 (IHC)
Anti-NeuN	Mouse	Millipore	MAB377	AB_2298772	1:500 (IHC)

antibody incubation, tissue sections were rinsed with 1% tris-buffered saline and incubated for 30 min with appropriate secondary antibodies (Table 2). This was followed by quenching with 3% hydrogen peroxide and a 30 min incubation with tertiary HRP label (BioLegend, cat: 93028). The immunocomplex was developed using diaminobenzidine as the chromogen (BioLegend, cat: SIG-31043-10), followed by light counterstaining with haematoxylin (Anatech Ltd, cat: 842). Slides were imaged using Leica DFC7000T microscope (Leica microsystems) at 20× objective. Tissue morphology was assessed by haematoxylin and eosin (H&E) staining (Fischer, Jacobson, Rose, & Zeller, 2008). The number of ionized calcium binding adaptor molecule 1 positive microglial cells was quantified manually, whereas the number of neuronal nuclei positive neurons was quantified using the ImageJ software (RRID: SCR_003070) (Abràmoff, Magalhães, & Ram, 2004). The immuno-related procedures used comply with the recommendations made by the *British Journal of Pharmacology* (Alexander et al., 2018).

2.8 | RNA extraction, reverse transcription and real-time (qRT)-PCR

Hippocampal tissues were lysed in TRIzol™ Reagent (ThermoFisher Scientific, cat: 15596018) and total RNA was extracted using a phenol-chloroform/iso-amyl alcohol step, followed by DNase 1 treatment, as previously described (Moidunny et al., 2016). Equal amounts (100 ng) of purified RNA were reverse transcribed to complementary DNA (cDNA) using the High-Capacity cDNA Reverse Transcription kit (ThermoFisher Scientific, cat: 4368814). Potential contamination of cDNA by genomic DNA was checked by running reactions without reverse transcriptase and using Gapdh primers (see Table 1 for primer sequences) for the subsequent PCR amplification. The relative gene expression was measured by real-time quantitative PCR on a LightCycler 96 machine (Roche). The expression of HIV-1 LTR, Bdnf, **Tnf- α** , **Il6**, **Cox-2** genes (see Table 1 for primer sequences) were measured using LightCycler 480 SYBR Green 1 Master Mix (Roche, cat: 4707516001), whereas the expression of Ngf, Ntf-3 and Ntf-4/5 genes were measured using TaqMan gene expression assays (Applied Biosystems) containing predesigned primers and probes (see Table 1) and LightCycler 480 Probes Master Mix (Roche, cat: 4707494001). The expression of housekeeping genes used for normalization, Rpl32 and Rps18, did not vary between mouse genotypes or treatments. The relative gene expression levels were calculated using the comparative C_t method (Livak & Schmittgen, 2001).

2.9 | Western blotting

Western blotting of hippocampal proteins was performed using LI-COR's Odyssey IR imaging system, as previously described (Moidunny et al., 2016). Briefly, whole hippocampus was transferred to a microcentrifuge tube containing radioimmunoprecipitation assay (RIPA) buffer (Sigma Aldrich, cat: R0278) supplemented with Halt™ Protease

and Phosphatase Inhibitor cocktail (ThermoFisher Scientific, cat: 78442). The tissues were homogenized using a mortar and pestle, sonicated and total proteins quantified using a bicinchoninic acid protein assay kit (ThermoFisher Scientific, cat: 23225), following manufacturer's instructions. Equal amounts of protein (35 μ g) were loaded onto 4–20% Mini-PROTEAN® TGX Stain-Free™ Protein Gels (Bio-Rad Laboratories, cat: 4568094) for electrophoresis and subsequently transferred to 0.45 μ m nitrocellulose membranes (Bio-Rad Laboratories, cat: 1620145). The membranes were blocked using Licor Odyssey blocking buffer (OBB, cat: 92740000; diluted 1:1 in PBS) for 2 h at room temperature and incubated overnight at 4°C with different combinations of primary antibodies (see Table 2 for the list of antibodies and the dilutions used) that were diluted in 1:1 odyssey blocking buffer and PBS-T (PBS + 0.1% Tween 20). Membranes were washed in PBT-T (4× 5 min) and incubated in the dark on an orbital shaker for 1 h at room temperature with appropriate fluorescent dye-conjugated secondary antibodies (see Table 2). Membranes were washed in PBS-T (4× 5 min) and fluorescent bands were detected using LI-COR's Odyssey IR imaging system. The sizes of proteins were verified by comparison with Precision Plus Protein™ All Blue Standards (Bio-Rad Laboratories, cat: 1610373). The densitometric analysis of protein bands was performed using Image Studio Lite Software (LI-COR Biosciences). Optical densities of target proteins were normalized to that of their loading controls and the value was expressed as “fold mean of the controls,” in order to compare across multiple experiments. The supporting information contains full images of all western blots used in this study. The experimental details of the western blot conform with the *British Journal of Pharmacology* guidelines (Alexander et al., 2018).

2.10 | BDNF ELISA

BDNF protein levels in tissue homogenates were measured using a mouse BDNF ELISA kit which recognizes mature BDNF (Abnova, cat: KA0331), following manufacturer's instructions.

2.11 | Data and statistical analysis

The data and statistical analysis comply with the recommendations of the *British Journal of Pharmacology* on experimental design and analysis in pharmacology (Curtis et al., 2018). Animals were randomly assigned for treatments and the experiments were designed to generate groups of equal sample size, except when there was a shortage in obtaining adequate numbers of age-matched mice, mainly due to the infanticidal behaviours in female Tg26 mice following the delivery of pups (see Section 2.1). Sample sizes were determined based on past experience and a previous publication that assessed learning and memory in Tg26 mice (Putatunda et al., 2019). The level of significance was set at 5% with 80% power to get minimum possible number of mice required for the experiment. Statistical analysis was undertaken only for experiments with a sample size of at least $n = 5$

per group. For experiments with a smaller sample size (i.e., $n < 5$), data are presented as preliminary observations. The group size is the number of independent values and the statistical analysis was done using these independent values. Blinding approaches were undertaken for electrophysiology, behavioural studies, TDZD-8 experiments as well as for the analysis of immunohistochemistry data. All data were analysed using GraphPad Prism software (version 5.02; GraphPad Software Inc., La Jolla, CA, USA; RRID:SCR_002798) and the results are presented as mean \pm SEM. Outliers were included in data analysis. Unpaired Student's *t*-tests and two-way ANOVA with Bonferroni or Tukey post hoc tests were used for group comparison. Post hoc tests were conducted only if *F* in ANOVA achieved $P < 0.05$. Parametric tests were performed after testing for normal distribution and confirming that there was no significant variance in homogeneity. Normalization of western blot data was employed in order to compare across multiple experiments (see Section 2.9 for details). Statistical significance was set at $P < 0.05$.

2.12 | Materials

TDZD-8 was purchased from Tocris Bioscience (cat: 6092). Tween-80, Tween-20, DMSO, isoflurane, sucrose, NaCl, KCl, NaH_2PO_4 , NaHCO_3 , MgCl_2 , CaCl_2 , D-glucose, paraformaldehyde, xylene, ethanol, PBS, tris-buffered saline, hydrogen peroxide, phenol, chloroform and isoamyl alcohol were purchased from Sigma Aldrich (St. Louis, MO, USA). Table 1 provides a list of primers and TaqMan assay probes used for qRT-PCR and genomic DNA PCR. Details of primary and secondary antibodies used for western blotting and immunohistochemistry are listed in Table 2.

2.13 | Nomenclature of targets and ligands

Key protein targets and ligands in this article are hyperlinked to corresponding entries in the IUPHAR/BPS Guide to PHARMACOLOGY <http://www.guidetopharmacology.org> and are permanently archived in the Concise Guide to PHARMACOLOGY 2019/20 (Alexander et al., 2019).

3 | RESULTS

3.1 | Male Tg26 mice show deficient contextual fear memory

We first established that neither male nor female Tg26 mice display overt deficiencies in basic strength, gross motor or sensory (visual and tactile) reflexes compared to their respective WT controls (Table 3). However, both male and female Tg26 mice had lower body weights than their WT counterparts (Table 3). Next, learning and memory of WT and Tg26 mice were assessed using the fear conditioning paradigm (Maren, Phan, & Liberzon, 2013). In the five inter-trial intervals during the conditioning session, freezing progressively ascended similarly between WT and Tg26 mice for both males and females (Figure 1a,c, respectively). Male Tg26 mice compared to male WT mice displayed a selective deficit in the contextual fear memory when tested 24 h after the conditioning session (Figure 1b). Notably, while both genotypes displayed greater freezing in the conditioned context as compared to baseline, male WT mice did so to a far greater extent than male Tg26 mice (WT male 51.86% vs. 18.53%; Tg26 male 33.07% vs. 20.33%). In contrast, both female Tg26 and WT mice showed similar increase in context-specific freezing compared to baseline freezing (Figure 1d). Response to the discrete cue paired with foot-shocks was similar between Tg26 and WT mice for both males and females (Figure 1b,d), indicating that this amygdala-related task was not affected in male and female Tg26 mice.

3.2 | Male Tg26 mice show impaired hippocampal basal synaptic transmission and LTP

We next performed electrophysiology in acute hippocampal slices to determine whether the sex-dependent contextual fear memory deficits in Tg26 mice were due to an alteration in hippocampal synaptic plasticity. Input–output responses at the Schaffer collateral-CA1 synapse revealed a significant reduction in fEPSPs at higher current intensities (160, 180 and 200 μA) in male Tg26 mice as compared to male WT mice (Figure 2a). In contrast, input–output responses of female Tg26 mice were similar to that of female WT mice (Figure 2d). In

TABLE 3 Tg26 mice show no overt deficits in sensory and motor functions

Genotype	Sex	Body weight (g)	Body temp. ($^{\circ}\text{C}$)	Spontaneous activity	Righting reflex	Bite irritability	Pupil reflex	Visual reflex	Grip strength	Wire maneuver
WT	Male	37.4 \pm 1.35	36.8 \pm 0.16	2.2 \pm 0.22	3.0	1.0 \pm 0.35	1.00 \pm 0.00	2.4 \pm 0.27	2.8 \pm 0.22	3.8 \pm 0.22
Tg26	Male	29.8 \pm 1.24*	36.9 \pm 0.15	2.8 \pm 0.22	3.0	1.2 \pm 0.42	1.00 \pm 0.00	2.8 \pm 0.22	2.2 \pm 0.22	3.4 \pm 0.45
WT	Female	26.0 \pm 1.25	36.9 \pm 0.28	2.8 \pm 0.29	3.0	2.8 \pm 0.29	0.75 \pm 0.17	2.5 \pm 0.33	2.0 \pm 0.00	3.0 \pm 0.00
Tg26	Female	22.3 \pm 0.73*	37.0 \pm 0.21	3.0 \pm 0.00	3.0	2.5 \pm 0.58	0.50 \pm 0.00	2.5 \pm 0.33	1.8 \pm 0.29	3.5 \pm 0.58

Note: Male and female Tg26 and littermate WT mice were assessed for differences in physiological, sensory, motor and reflexive responses by a modified SmithKline Beecham, Harwell, Imperial College, Royal London Hospital Phenotype Assessment screen (see section 2.4 for scoring criteria used). Both male and female Tg26 mice had lower body mass compared to their respective WT controls. $n = 5$ per each group; unpaired Student's *t*-test. Data are presented as the mean \pm SEM.

* $P < 0.05$.

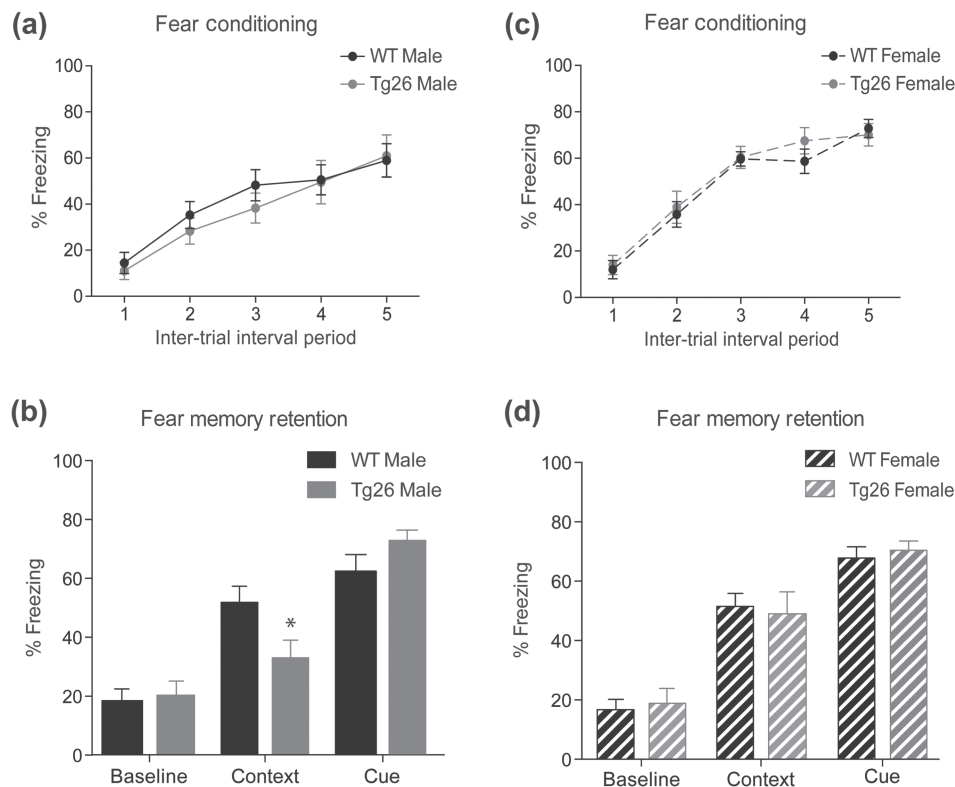


FIGURE 1 Impaired contextual fear memory in male, but not female, Tg26 mice. Male (a) and female (c) Tg26 and littermate WT mice were put through a delay fear conditioning paradigm consisting of discrete cues (80 dB white noise and dim house light) that were temporally paired with a foot-shock (0.7 mA, 1 sec) and diffuse contextual cues (standard test chamber with Simple Green scent) present throughout the conditioning session. Over the 5 cue-shock pairings mice displayed an increased freezing (fear) response following the shock. Fear memory was assessed in the male (b) and female (d) mice 24 h after the conditioning. Male Tg26 mice show normal baseline and cue-freezing (fear) in an altered context, but reduced fear in the context that was paired with foot-shock. * $P < 0.05$ as compared to WT, $n = 10$ for male WT, $n = 9$ for male Tg26, $n = 14$ for female WT and $n = 12$ for female Tg26 mice; two-way ANOVA with Bonferroni's correction. Cue-freezing behaviour was measured for 2 min during presentation of the shock-associated cues (80 dB white noise and dim house light) in a contextually altered test chamber. Data are expressed as per cent time the animal spends freezing. No differences in contextual- and cued-fear memories were observed between female WT and Tg26 mice

addition, analysis of fEPSPs after high frequency tetanization showed a significant reduction in hippocampal LTP in male Tg26 mice (Figure 2b) but not in female Tg26 mice (Figure 2e). Further analysis of the average fEPSP response from 0 to 5 min after tetanization showed no significant differences between genotypes in either male or female mice (Figure 2c,f). However, LTP expression was not maintained in male Tg26 mice when assessed at 45–60 min post tetanization (Figure 2c), whereas it remained potentiated in female Tg26 mice (Figure 2f). These results indicate that hippocampal basal synaptic transmission and LTP are impaired in male, but not female, Tg26 mice.

3.3 | Male Tg26 mice show increased hippocampal HIV-1 LTR mRNA expression, reduced BDNF mRNA and protein and reduced synapsin-1 and phospho-Ser831 GluA1 protein levels

We next investigated the mechanisms underlying impaired hippocampal synaptic plasticity and reduced cognition in male Tg26 mice. First,

we confirmed HIV-1 proviral DNA expression in Tg26 mouse brain by PCR (Figure 3a). HIV-1 LTR, *tat* and *nef* were detected in the hippocampus of Tg26 mice but not in WT mice. Interestingly, hippocampal expression of HIV-1 LTR mRNA in male Tg26 mice was significantly higher by ~60% when compared to that of female Tg26 mice (Figure 3b). However, we did not observe any overt signs of hippocampal damage in male Tg26 mice with H&E staining (Figure 3c). In addition, the number of neuronal nuclei positive neurons in hippocampal CA1, CA3 and dentate gyrus areas of male Tg26 mice were similar to that of male WT mice (Figure 3c). Moreover, the number of ionized calcium binding adaptor molecule 1 positive microglia, the level of ionized calcium binding adaptor molecule 1 protein and the expression of *Tnf- α* , *Il6* and *Cox-2* mRNA were unaltered in male Tg26 mice when compared to that of male WT mice (Figure 3c–g). Interestingly, we observed a 23% reduction in hippocampal BDNF mRNA (Figure 4a) and a 21% reduction in BDNF protein level (Figure 4b) in male Tg26 mice compared to male WT mice, whereas the expression of BDNF mRNA in the amygdala was unaltered in male Tg26 mice compared to male WT mice (Figure 4c). Additionally, we observed that the hippocampal expression of *Ngf*, *Ntf-3* and *Ntf-4/5* mRNA (Figure 4d–f) and

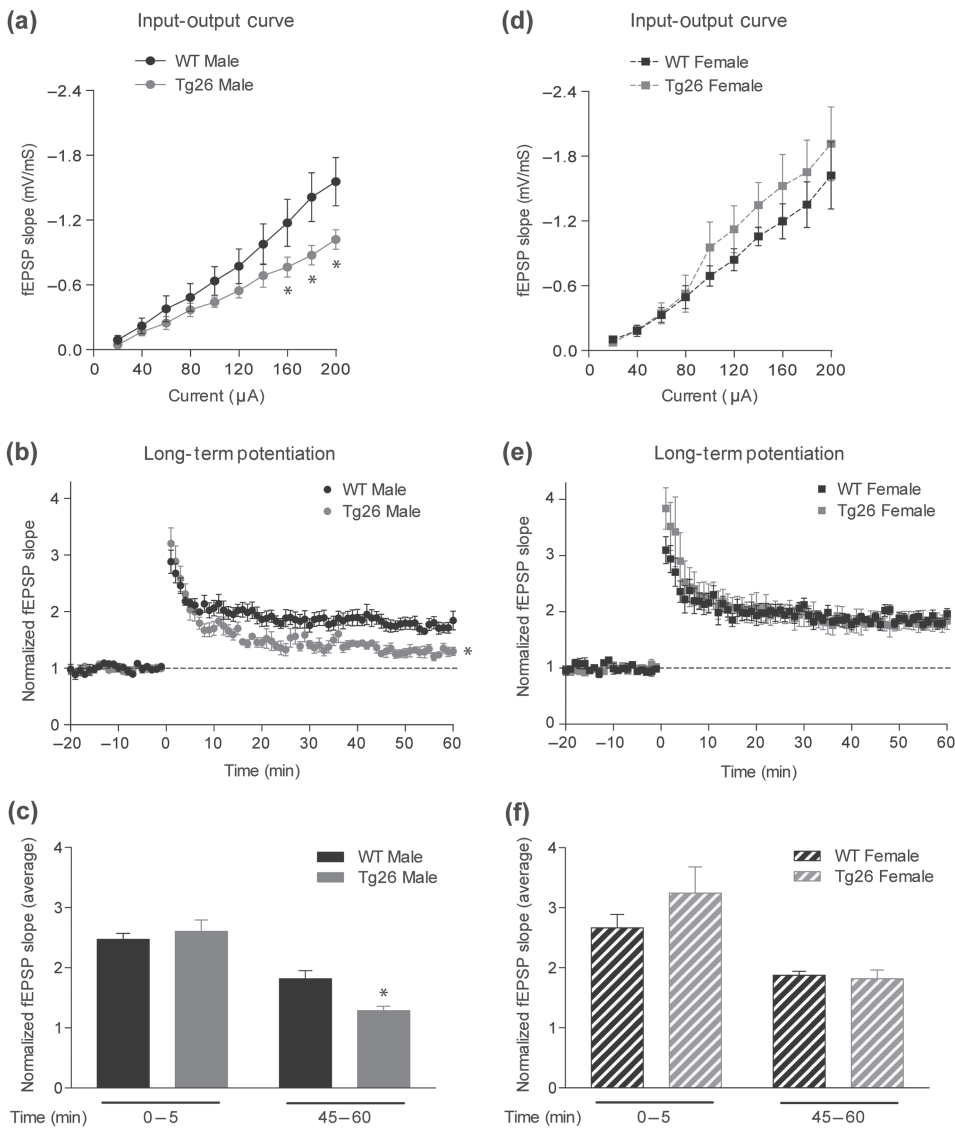


FIGURE 2 Male, but not female, Tg26 mice show impaired hippocampal basal synaptic transmission and long-term potentiation (LTP). Input-output (IO) responses from male (a) and female (d) Tg26 and littermate WT mice ($n = 6$ per each group). IO responses were significantly reduced in male Tg26 mice, but not in female Tg26 mice as compared to their respective WT controls. $*P < 0.05$ as compared to WT; repeated measures two-way ANOVA with Tukey's HSD correction. LTP induced by high frequency tetanization from male (b) and female (e) mice. LTP was significantly impaired in male Tg26 mice as compared to WT mice, but normal in female Tg26 mice. $*P < 0.05$ as compared to WT, repeated measures two-way ANOVA with Tukey's HSD correction. Average of fEPSP slopes from 0 to 5 min and 45–60 min post-tetanzation from male (c) and female (f) mice. $*P < 0.05$ as compared to WT 45–60 min; two-way ANOVA with Tukey's HSD correction

the levels of BDNF receptor (TrkB and p75NTR) proteins (Figure 4g) were unaltered in male Tg26 mice. Of note, preliminary observations indicated that the hippocampal BDNF mRNA and protein levels were unaltered in female Tg26 mice when compared to that of female WT mice (Figure 4h–i).

Further analysis of hippocampal pre- and post-synaptic proteins revealed a significant reduction in synapsin-1 level by 25.55% in male Tg26 mice compared to male WT mice (Figure 5a), whereas the synapsin-1 protein level was unaltered in female Tg26 mice compared to female WT mice (Figure 5a). Next, analysis of the hippocampal phospho-Ser831 AMPA glutamate receptor (GluA1) protein level after fear conditioning showed a significant 57.59% increase in male WT mice and a 37.2% decrease in male Tg26 mice (Figure 5b). Taken together, these results indicate that the reduced hippocampal synapsin-1, phospho-Ser831 GluA1 and BDNF levels, but not neuroinflammation or neuronal loss, may underlie the synaptic plasticity deficits and cognitive impairments observed in male Tg26 mice.

3.4 | GSK3 inhibition increases hippocampal phospho-Ser831 GluA1, synapsin-1 and BDNF protein levels, rescues deficits in hippocampal basal synaptic transmission and LTP, and improves contextual fear memory in male Tg26 mice

Overexpression of constitutively active GSK3 β , an isoform of GSK3 which is abundantly expressed in the hippocampus (Pandey et al., 2009), causes significant reduction in neuronal synapsin-1 expression (Zhu et al., 2007), whereas inhibition of GSK3 increases synapsin expression in cultured neurons and BDNF expression in the hippocampus (Cuesto et al., 2015; Fukumoto, Morinobu, Okamoto, Kagaya, & Yamawaki, 2001). In addition, ketamine, which inhibits GSK3, increases hippocampal membrane level of GluA1 protein (Beurel, Grieco, Amadei, Downey, & Jope, 2016), suggesting that GSK3 might be responsible for the reduced synapsin-1, BDNF and phospho-Ser831 GluA1 levels in male Tg26 mice. Consistently, we observed a $\sim 26\%$ reduction in the phospho-Ser9 GSK3 β /GSK3 β

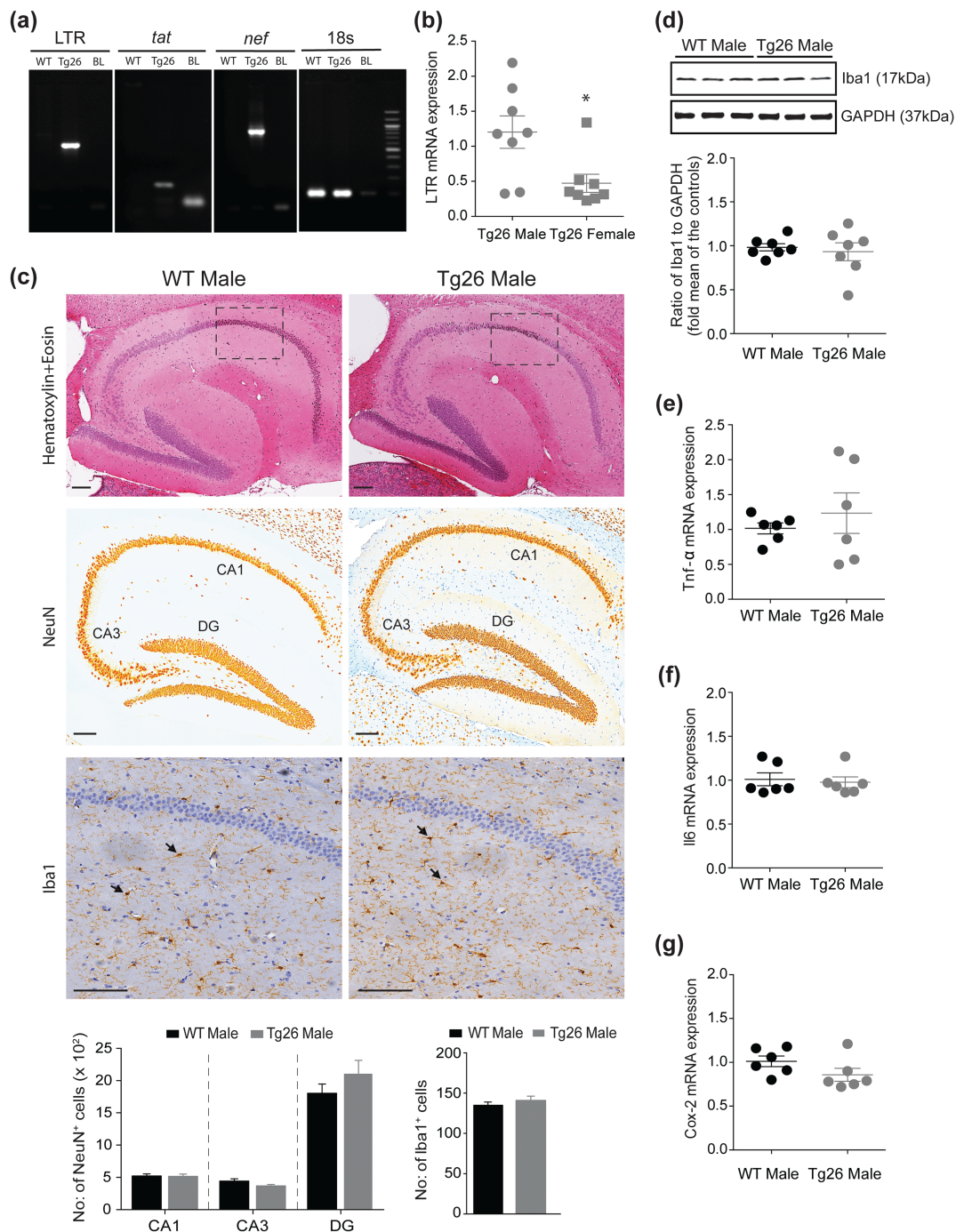


FIGURE 3 Male Tg26 mice show increased hippocampal expression of HIV-1 long terminal repeat (LTR) mRNA, which did not result in neuronal loss and microglial activation. (a) PCR reactions on total genomic DNA isolated from hippocampal brain regions show specific bands for HIV-1 LTR, *tat* and *nef* in Tg26, but not in WT, mouse. Equal sized bands were detected for 18s, which served as housekeeping control. (b) qRT-PCR analysis of hippocampal HIV-1 LTR gene in male and female Tg26 mice ($n = 8$ per group). * $P < 0.05$, unpaired Student's *t*-test. (c) Immunohistochemistry of paraffin-embedded sagittal sections of hippocampal brain region of male WT and Tg26 mice. Representative images of haematoxylin and eosin staining (top panel) shows no overt signs of pathology. Representative images of anti-neuronal nuclei (NeuN) and anti-ionized calcium binding adaptor molecule 1 (Iba1) immunostaining (middle and bottom panels, respectively) and analyses (histograms) show similar numbers of NeuN positive neurons (in areas CA1, CA3 and dentate gyrus (DG)) and Iba1 positive microglial cells between male WT and Tg26 mice. Insets in the top panel indicate area of selection for representative Iba1 images. Black arrow heads (bottom panels) indicate Iba1 positive microglial cells. Scale bar 50 μm , $n = 6$ for WT mice (average of four brain sections per mouse) and $n = 5$ for Tg26 mice (average of six brain sections per mouse). (d) Representative western blots and densitometric analysis of Iba1 protein (17 kDa) showing similar hippocampal levels between male WT and Tg26 mice ($n = 7$ per group). GAPDH (37 kDa) served as loading control. (e-g) qRT-PCR analysis of hippocampal Tnf- α , Il6 and Cox-2 mRNA showing similar gene expression between male WT and Tg26 mice ($n = 6$ per group)

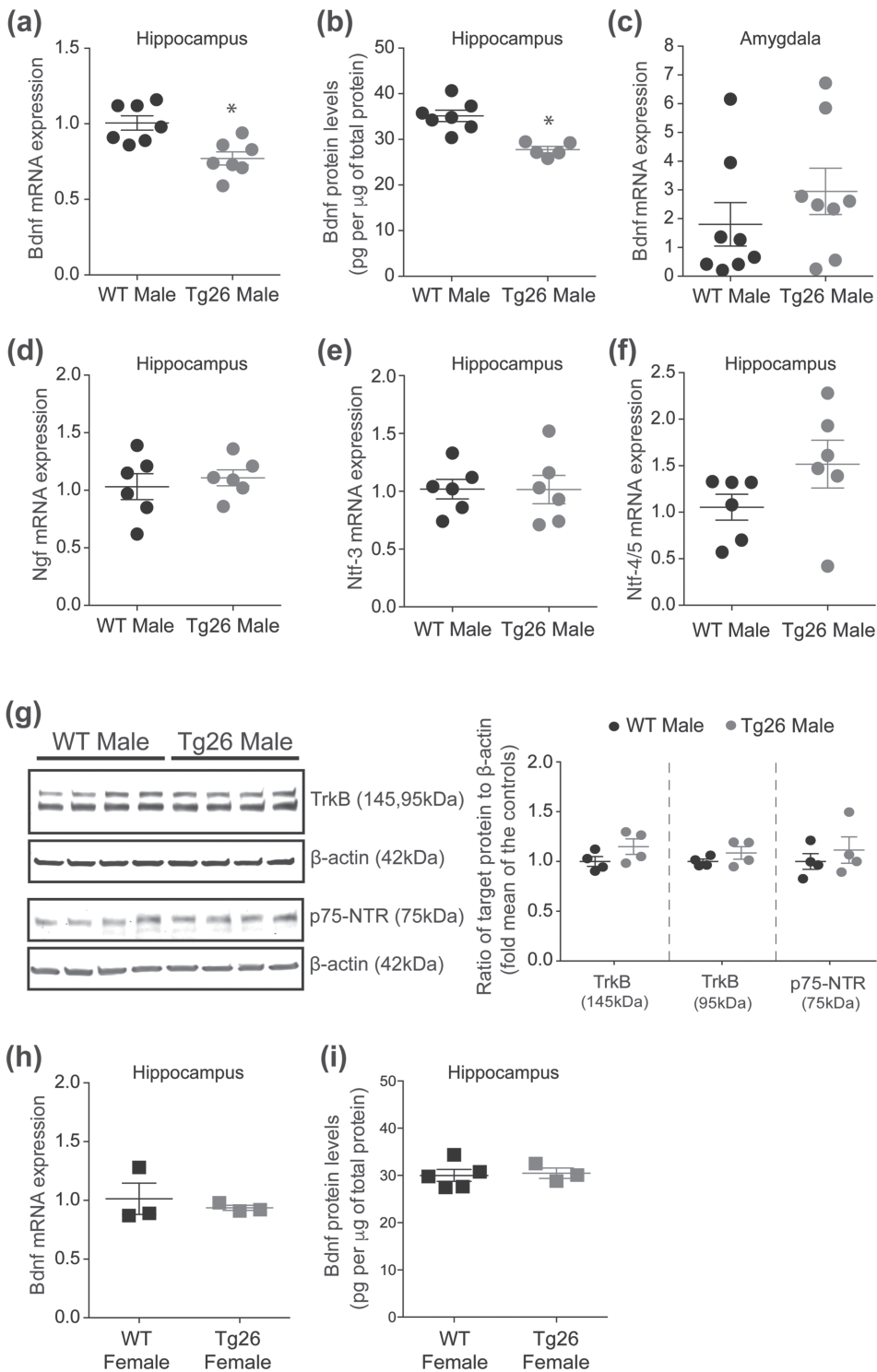


FIGURE 4 Male, but not female, Tg26 mice show reduced hippocampal BDNF mRNA and protein levels. (a) qRT-PCR analysis of hippocampal BDNF mRNA in male WT and Tg26 mice ($n = 7$ per group) and (b) ELISA analysis of hippocampal BDNF protein in male WT and Tg26 mice ($n = 7$ for WT, $n = 5$ for Tg26). A significant reduction in hippocampal BDNF mRNA and protein was observed in male Tg26 mice. * $P < 0.05$ as compared to WT, unpaired Student's *t*-test. (c) qRT-PCR analysis of BDNF mRNA in amygdala showing similar expression between male WT and Tg26 mice ($n = 8$ per group). (d–f) qRT-PCR analysis of hippocampal Ngf, Ntf-3 and Ntf-4/5 mRNA, respectively, showing similar expression between male WT and Tg26 mice ($n = 6$ per group). Rps18 served as housekeeping gene. (g) Representative western blots and densitometric analysis of TrkB and p75-NTR proteins showing similar levels of full length (145 kDa) and truncated (95 kDa) forms of the TrkB receptor and p75-NTR (75 kDa) receptor proteins in male Tg26 and WT mice ($n = 4$ per group). β -actin (42 kDa) served as loading control. (h) qRT-PCR analysis of hippocampal BDNF mRNA in female WT and Tg26 mice ($n = 3$ per group) and (i) ELISA analysis of hippocampal BDNF protein in female WT and Tg26 mice ($n = 5$ for WT, $n = 3$ for Tg26), showing similar levels between the two genotypes

protein ratio, indicating increased GSK3 β activity (Sutherland, Leighton, & Cohen, 1993), in male Tg26 mice compared to male WT mice (Figure 5c). The hippocampal level of total GSK3 proteins was similar between male Tg26 mice and male WT mice (Figure 5c). We next investigated whether selective inhibition of GSK3 β using TDZD-8 would rescue the molecular and synaptic deficits observed in male Tg26 mice. TDZD-8 treatment (5 mg·kg $^{-1}$ for 24 h) did not

alter the total levels of GSK3 β protein, but it significantly increased phospho-Ser9 GSK3 β /GSK3 β protein ratio, in both male WT and Tg26 mice (Figure 6a). Excitingly, TDZD-8 treatment increased hippocampal levels of phospho-Ser831 GluA1 protein by 94.4% and synapsin-1 protein by 29.5% in male Tg26 mice when compared to the saline treated male Tg26 mice (Figure 6b). These effects of TDZD-8 were absent in the WT mice (Figure 6b). In addition, TDZD-8

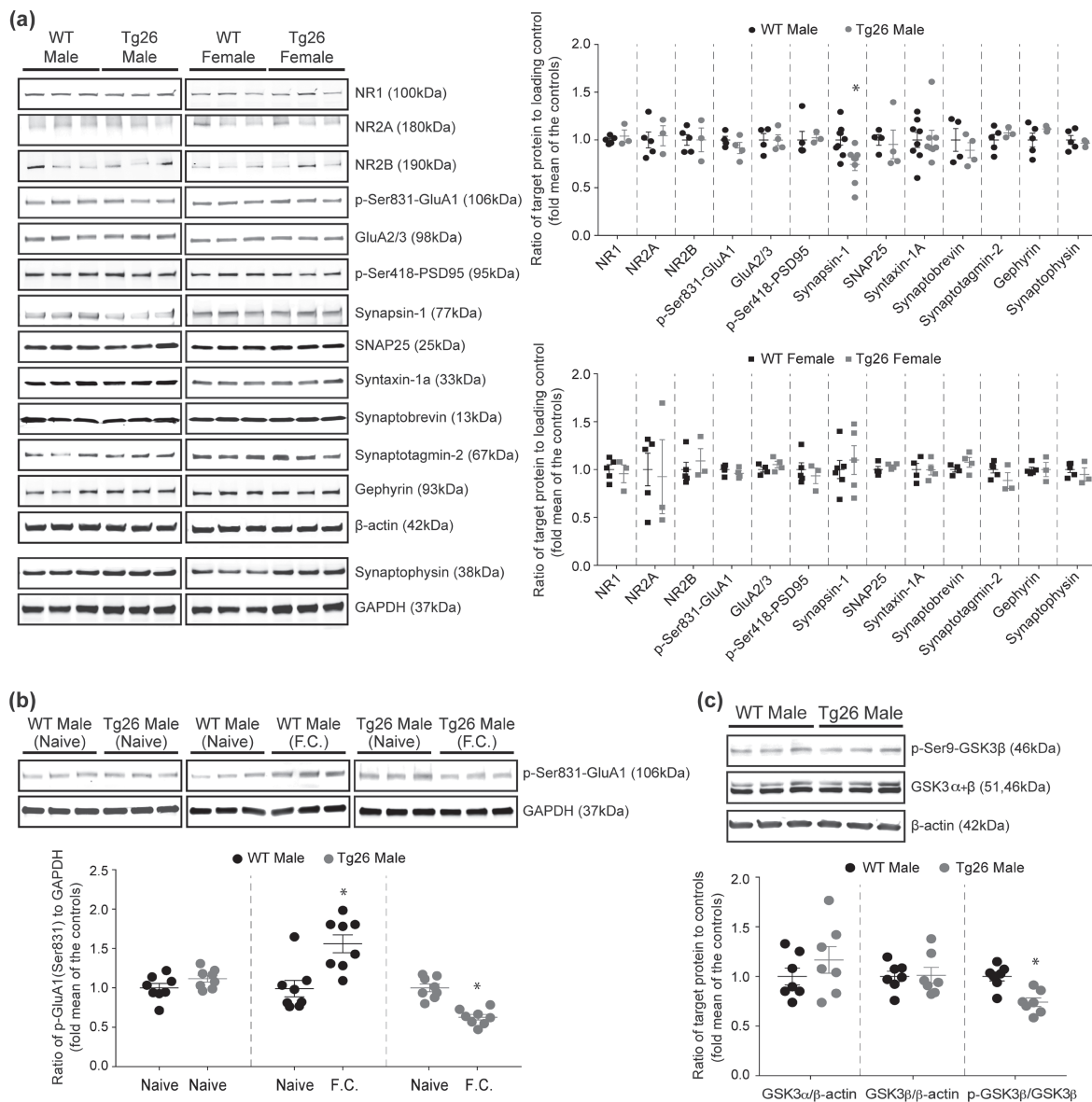


FIGURE 5 Male Tg26 mice show reduced hippocampal synapsin-1 levels, decreased GluA1 phosphorylation post fear conditioning and increased hippocampal GSK3 β activity. (a) Representative western blots and densitometric analyses of hippocampal pre- and post-synaptic proteins in male and female WT and Tg26 mice. A significant reduction in synapsin-1 proteins (77 kDa) was observed in male, but not female, Tg26 mice compared to the WT mice. $n = 9$ for male WT, $n = 8$ for male Tg26, $n = 6$ for female WT, $n = 5$ for female Tg26; $*P < 0.05$ as compared to WT, unpaired Student's *t*-test. The levels of NR1 (100 kDa; $n = 5$ for male WT, $n = 3$ for male Tg26, $n = 5$ for female WT, $n = 3$ for female Tg26), NR2A (180 kDa; $n = 5$ for male WT, $n = 3$ for male Tg26, $n = 5$ for female WT, $n = 3$ for female Tg26), NR2B (190 kDa; $n = 5$ for male WT, $n = 3$ for male Tg26, $n = 5$ for female WT, $n = 3$ for female Tg26), phospho-Ser831 GluA1 (106 kDa; $n = 4$ per each group), GluA2/3 (98 kDa; $n = 4$ per each group), phospho-Ser418 PSD95 (95 kDa; $n = 5$ for male WT, $n = 3$ for male Tg26, $n = 5$ for female WT, $n = 3$ for female Tg26), SNAP25 (25 kDa; $n = 4$ per each group), syntaxin-1a (33 kDa; $n = 8$ for male WT, $n = 8$ for male Tg26, $n = 4$ for female WT, $n = 4$ for female Tg26), synaptobrevin (13 kDa; $n = 4$ per each group), synaptotagmin-2 (67 kDa; $n = 5$ for male WT, $n = 3$ for male Tg26, $n = 5$ for female WT, $n = 3$ for female Tg26), gephyrin (93 kDa; $n = 5$ for male WT, $n = 3$ for male Tg26, $n = 5$ for female WT, $n = 3$ for female Tg26) and synaptophysin (38 kDa; $n = 5$ for male WT, $n = 3$ for male Tg26, $n = 5$ for female WT, $n = 3$ for female Tg26) proteins were unaltered in male and female Tg26 mice as compared to their respective WT controls. β -actin (42 kDa) and GAPDH (37 kDa) served as loading controls. (b) Representative western blots and densitometric analysis of hippocampal phospho-Ser831 GluA1 protein in naïve and fear conditioned male WT and Tg26 mice ($n = 8$ per each group). Naïve WT and Tg26 mice showed similar levels of phospho-Ser831 GluA1 proteins, which increased significantly in WT mice 30 min after fear conditioning. In contrast, male Tg26 mice showed a significant reduction in phospho-Ser831 GluA1 levels post fear conditioning. $*P < 0.05$ as compared to naïve group, unpaired Student's *t*-test. (c) Representative western blots and densitometric analysis of hippocampal total GSK3 α (51 kDa), total GSK3 β (46 kDa) and phospho-Ser9-GSK3 β (46 kDa; inactive form) proteins in male WT and Tg26 mice ($n = 7$ per each group). Analysis of phospho-Ser9-GSK3 β /GSK3 β ratio showed a significant reduction in male Tg26 mice compared to male WT mice. $*P < 0.05$, unpaired Student's *t*-test. Analysis of GSK3 α / β -actin and GSK3 β / β -actin ratios showed similar levels between male Tg26 and WT mice. β -actin (42 kDa) served as loading control

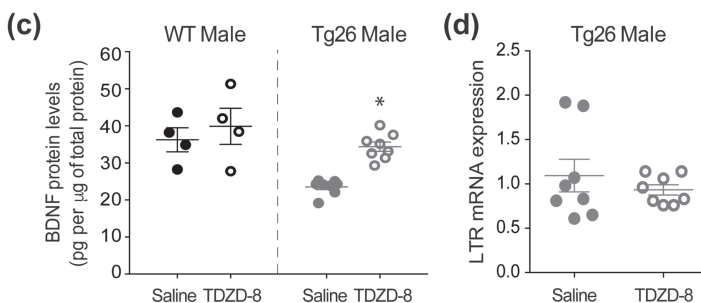
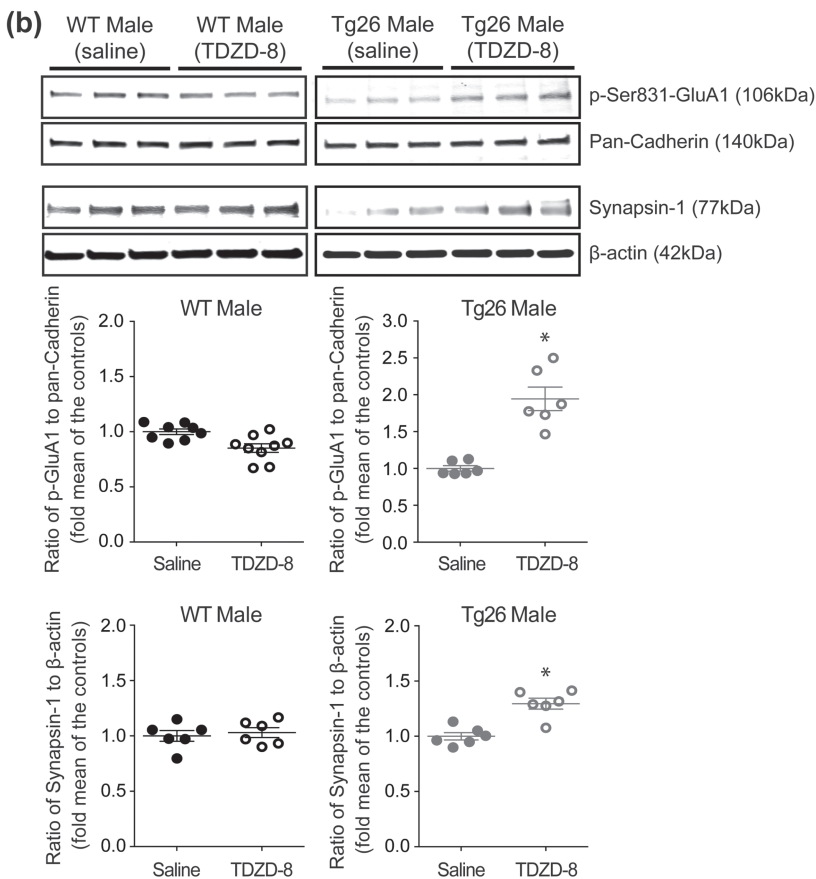
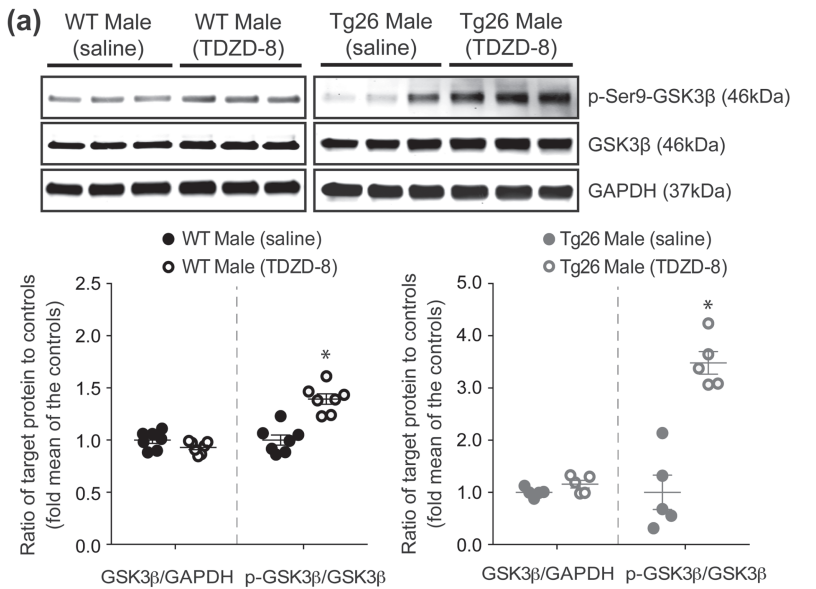


FIGURE 6 GSK3 inhibition increases hippocampal levels of phospho-Ser831 GluA1, synapsin-1 and BDNF proteins in male Tg26 mice. (a) Representative western blots and densitometric analyses showing the effect of saline and GSK3 inhibitor (TDZD-8; 5 mg·kg⁻¹ for 24 h) treatments on hippocampal total GSK3β (46 kDa) and phospho-Ser9-GSK3β (46 kDa; inactive form) proteins in male WT and Tg26 mice (*n* = 7 per group for saline and TDZD-8 treated WT; *n* = 5 per group for saline and TDZD-8 treated Tg26). Analysis of the phospho-Ser9-GSK3β/GSK3β ratios showed a significant increase in both male WT and Tg26 mice following TDZD-8 treatment. **P* < 0.05, unpaired Student's *t*-test. Analysis of total GSK3β/GAPDH ratios showed similar levels between saline and TDZD-8 treated mice. GAPDH (37 kDa) served as loading control. (b) Representative western blots and densitometric analyses showing the effect of saline and TDZD-8 treatments on hippocampal levels of phospho-Ser831 GluA1 (106 kDa; *n* = 8 per group for saline treated WT, *n* = 9 per group for TDZD-8 treated WT, *n* = 6 per group for saline treated Tg26, *n* = 6 per group for TDZD-8 treated Tg26) and synapsin-1 (77 kDa; *n* = 6 per treatment group for WT and Tg26) proteins in male WT and Tg26 mice. Pan-Cadherin (140 kDa) and β-actin (42 kDa) served as loading controls. **P* < 0.05, as compared to saline-treated mice, unpaired Student's *t*-test. (c) ELISA analysis of hippocampal BDNF proteins in male WT and Tg26 mice following saline and TDZD-8 treatments (*n* = 4 per treatment group for WT and *n* = 8 per treatment group for Tg26). **P* < 0.05, as compared to saline-treated mice, unpaired Student's *t*-test. (d) qRT-PCR analysis of hippocampal HIV-1 long terminal repeat (LTR) mRNA in saline and TDZD-8 treated male Tg26 mice (*n* = 8 per treatment group)

treatment significantly increased hippocampal BDNF protein level in male Tg26 mice, but not in male WT mice (Figure 6c). TDZD-8 treatment did not alter hippocampal HIV-1 LTR mRNA expression in male Tg26 mice, when compared to the saline treated controls (Figure 6d).

We next investigated whether TDZD-8 treatment would rescue the deficits in hippocampal synaptic plasticity in male Tg26 mice. TDZD-8 treatment did not affect the input–output responses of male WT mice, but significantly improved the input–output responses of male Tg26 mice (Figure 7a). In addition, TDZD-8 treatment rescued the observed LTP deficits in male Tg26 mice (Figure 7b). Further analysis of the fEPSP slope revealed that TDZD-8 treatment did not alter post-tetanic potentiation and short-term potentiation (0–5 min after tetanization) in male WT or Tg26 mice but maintained the expression of LTP (45–60 min after tetanization) in male Tg26 mice (Figure 7c). Finally, we measured the effect of TDZD-8 treatment on behavioural responses of mice. Both saline and TDZD-8 treated male WT and Tg26 mice displayed similar behavioural responses (flinch, hop, run and jump) to increasing shock intensities (Figure 7d), indicating that the drug treatment did not alter sensitivity of mice to shock. However, TDZD-8 treated male WT and Tg26 mice compared to saline treated controls showed elevated freezing responses at various inter-trial interval periods during the fear conditioning session (Figure 7e). Excitingly, TDZD-8 treatment significantly improved the contextual fear memory of male Tg26 mice as compared to the saline treated male Tg26 mice (Figure 7f). Of note, TDZD-8 treatment neither affected the contextual fear memory of male WT mice (Figure 7f) nor altered the baseline fear response and cue-dependent memory in either of the genotypes when compared to their respective saline-treated controls (Figure 7f). Finally, the magnitude of contextual freezing in the TDZD-8 treated male Tg26 mice was similar to that of the saline-treated male WT mice, indicating a complete restoration of contextual fear memory in male Tg26 mice after TDZD-8 treatment.

4 | DISCUSSION

Impairments in episodic memory are commonly observed in HIV-1 patients treated with antiretroviral therapy (Goodkin et al., 2017). In this study, we investigated the role of biological sex in the development of episodic memory deficits in HIV-1 Tg26 mice, using a fear conditioning paradigm. We showed that male, but not female, Tg26 mice exhibit impaired contextual fear memory, whereas no apparent deficits in cued-fear memory were observed in male or female Tg26 mice compared to their respective WT controls. These findings are indicative of hippocampal synaptic plasticity deficits in male Tg26 mice (Maren, Phan, & Liberzon, 2013). In accordance, a recent study of middle-aged Tg26 mice reported spatial memory deficits, although episodic memory was not affected at that age (Putatunda et al., 2019). We demonstrated that the contextual fear memory deficits in male Tg26 mice were not associated with changes in number of hippocampal neurons or microglia. In addition, we showed that the cognitive deficits were independent of microglial activation (Iba1

protein level) or induction of pro-inflammatory mediators such as Tnf- α , Il6 and Cox-2. Although neuroinflammation has been described to play a crucial role in HAND pathogenesis (McGuire, Gill et al., 2015), our findings are in accordance with those observed in the HIV-1 trans-activator of transcription (Tat) transgenic mice, which showed profound deficits in contextual fear memory in the absence of pyramidal neuron death (Fitting et al., 2013; Hahn et al., 2015). Additionally, neurocognitive impairments and synaptic dysfunction observed in HIV-1 transgenic rats and EcoHIV (murine HIV)-infected mice were not associated with neuroinflammation (Kelschenbach et al., 2019; McLaurin, Li, Booze, & Mactutus, 2019). Therefore, we turned to electrophysiology to understand the circuitry changes that may underlie these hippocampal learning and memory deficits in Tg26 mice. Analysis of the hippocampal Schaffer collateral-CA1 synapse revealed significant impairments in basal synaptic transmission and LTP in male Tg26 mice as compared to the male WT mice. Interestingly, both basal synaptic transmission and LTP were unaltered in female Tg26 mice, corresponding to no apparent deficits in their contextual fear memory. In addition, we found a significant decrease in the hippocampal level of phospho-Ser831 GluA1 proteins in male Tg26 mice post fear conditioning. Together with the finding that hippocampal LTP, but not post-tetanic potentiation or short-term potentiation, is impaired these results suggest that protein kinase or phosphatase signalling pathways are altered in male Tg26 mice, leading to impaired post-synaptic glutamate receptor activation during hippocampal LTP and learning.

Altered levels of BDNF, an important regulator of glutamate receptor activation, neurotransmitter release, hippocampal LTP and memory, have been widely implicated in HAND pathogenesis (Bachis, Avdoshina, Zecca, Parsadanian, & Mocchetti, 2012; Fields, Dumaop, Langford, Rockenstein, & Masliah, 2014; Jovanovic, Czernik, Fienberg, Greengard, & Sihra, 2000; Leal, Comprido, & Duarte, 2014). In this study, we demonstrated that the deficits in hippocampal LTP and contextual fear memory in male Tg26 mice were associated with a significant reduction in hippocampal BDNF mRNA and protein levels. We also demonstrated that BDNF mRNA expression in the amygdala was unaltered in male Tg26 mice, which corresponded to the unaltered amygdala-dependent cued fear memory in these animals. Furthermore, we showed a significant reduction in the hippocampal level of synapsin-1, a pre-synaptic phosphoprotein that regulates BDNF-induced neurotransmitter release, in male Tg26 mice (Jovanovic, Czernik, Fienberg, Greengard, & Sihra, 2000). Interestingly, hippocampal BDNF and synapsin-1 levels were unaltered in female Tg26 mice. Collectively, these findings imply that male Tg26 mice may have deficits in pre-synaptic glutamate release mechanisms in addition to the post-synaptic impairments. It is unclear what causes the reduction of hippocampal BDNF and synapsin-1 selectively in the male Tg26 mice. There is evidence indicating that a reduction in synapsin-1 levels in synaptosomes isolated from the frontal neocortex of HIV-1 infected humans corresponds to HIV-1 viral load in the brain (Gelman & Nguyen, 2010). In accordance, we observed a threefold higher expression of HIV-1 LTR mRNA in hippocampus of male Tg26 mice compared to the female Tg26 mice, suggesting that the selective

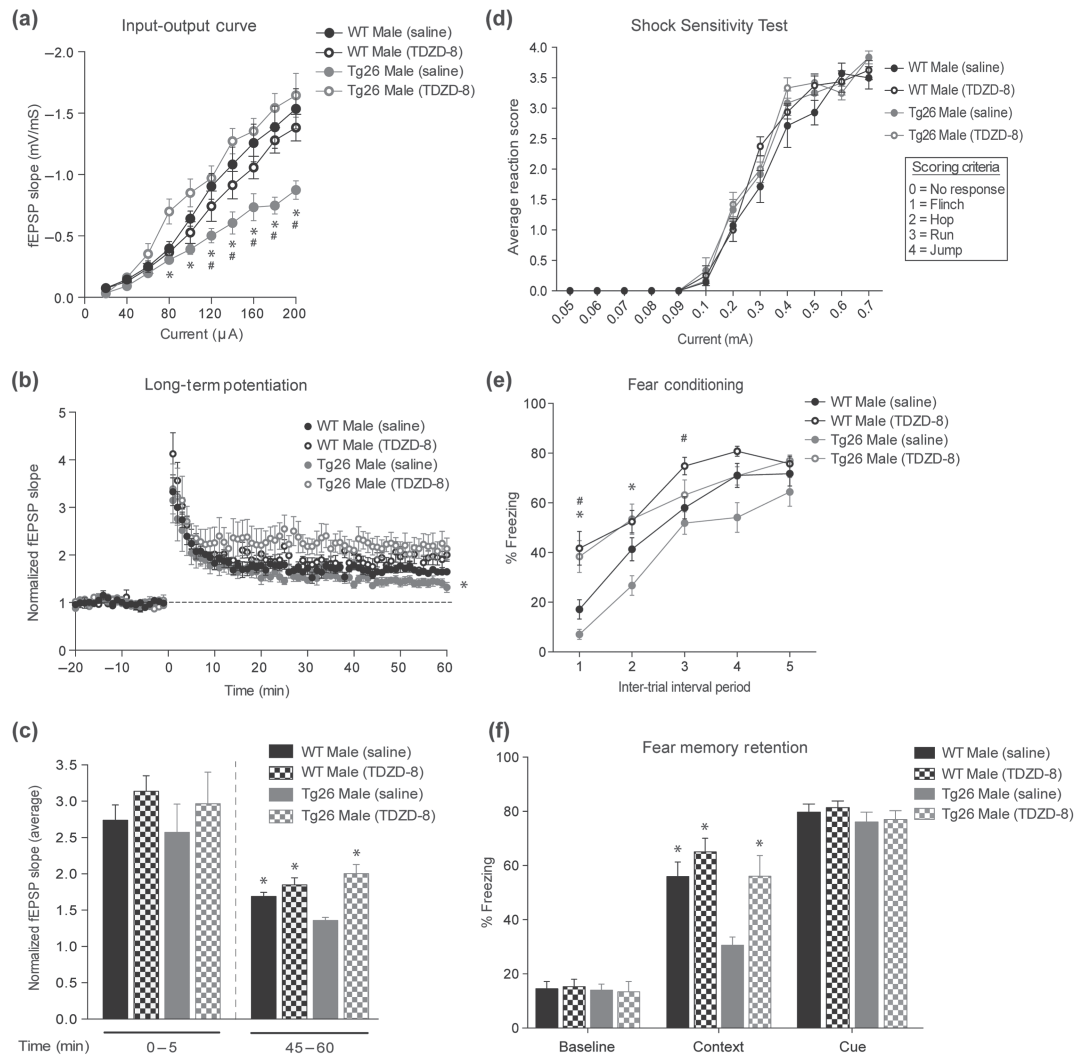


FIGURE 7 GSK3 inhibition rescues the deficits in basal hippocampal synaptic transmission, long-term potentiation (LTP) and contextual fear memory in male Tg26 mice. (a) Input–output (IO) curves showing significant improvement in hippocampal fEPSPs in male Tg26 mice following treatment with GSK3 inhibitor (TDZD-8; $5 \text{ mg} \cdot \text{kg}^{-1}$ for 24 h) as compared to male Tg26 mice treated with saline ($n = 5$ for saline treated WT, $n = 5$ for TDZD-8 treated WT, $n = 6$ for saline treated Tg26, $n = 5$ for TDZD-8 treated Tg26). * $P < 0.05$, for Tg26 male saline vs. TDZD-8; # $P < 0.05$, for Tg26 male saline vs. WT male saline, repeated measures two-way ANOVA with Tukey's HSD correction. (b) TDZD-8 treatment rescued the LTP deficits in male Tg26 mice as compared to the saline treated Tg26 mice ($n = 5$ for saline treated WT, $n = 5$ for TDZD-8 treated WT, $n = 6$ for saline treated Tg26, $n = 5$ for TDZD-8 treated Tg26). * $P < 0.05$ for Tg26 male saline vs. TDZD-8, repeated measures two-way ANOVA with Tukey's HSD correction. (c) Average of fEPSP slopes from 0 to 5 min and 45–60 min post-tetanzation. * $P < 0.05$, as compared to Tg26 male saline, two-way ANOVA with Tukey's HSD correction. (d) Shock-sensitivity test showing similar response of male WT and Tg26 mice to foot-shock following saline and TDZD-8 treatments. The flinch, hop, run and jump responses of mice to increasing current (0.05–0.7 mA) were scored on a scale of 0–4 (see inset for scoring criteria), as previously described (Nielsen & Crnic, 2002). Each data point is an average of responses of eight mice per treatment group for WT mice and six mice per treatment group for Tg26 mice. (e) Per cent freezing response of male WT and Tg26 mice during fear conditioning 30 min after saline or TDZD-8 treatment ($n = 16$ for saline treated WT, $n = 11$ for TDZD-8 treated WT, $n = 9$ for saline treated Tg26 and $n = 11$ for TDZD-8 treated Tg26). Over the five cue-shock pairings mice displayed an increased freezing (fear) response following the shock. TDZD-8 treated WT and Tg26 mice showed increased freezing response during the initial inter-trial intervals when compared to saline treated controls. * $P < 0.05$, for Tg26 male saline vs. TDZD-8; # $P < 0.05$, for WT male saline vs. TDZD-8, repeated measures two-way ANOVA with Tukey's HSD correction. (f) Fear memory response of saline and TDZD-8 treated male WT and Tg26 mice 24 h after the conditioning ($n = 16$ for saline treated WT, $n = 11$ for TDZD-8 treated WT, $n = 9$ for saline treated Tg26 and $n = 11$ for TDZD-8 treated Tg26). Both WT and Tg26 mice, irrespective of treatments, showed similar baseline- and cue-freezing in an altered context. In male Tg26 mice, TDZD-8 treatment significantly improved contextual fear memory compared to saline treatment. * $P < 0.05$, as compared to Tg26 male saline, two-way ANOVA with Bonferroni's correction. No significant difference in contextual fear memory was observed between saline and TDZD-8 treated male WT mice. Data are expressed as % time the animal spends freezing

reduction of synapsin-1 levels in male Tg26 mice may be a consequence of increased expression of HIV-1 proviral genes. We speculate that the lower HIV-1 LTR gene expression as well as intact cognition and BDNF levels in the female Tg26 mice are due to the neurotrophic actions of the endogenous steroid hormone **17 β -estradiol (E2)** (Das et al., 2018; Luine & Frankfurt, 2013). Future studies using ovariectomized female mice will determine whether the observed intact cognition in female Tg26 mice is due to a protective function of E2. In addition, since confounding factors of HAND such as psychiatric disorders and cerebrovascular disease are increasingly prevalent in older HIV-positive women (Chow et al., 2018; Robertson et al., 2014; Wisniewski et al., 2005), a longitudinal analysis of cognition in female Tg26 mice is important to determine the onset of cognitive decline in the females. Nevertheless, in this study, we show that male Tg26 mice compared to the female Tg26 mice display an earlier onset of neurocognitive decline, specifically in the hippocampal dependent contextual fear memory.

We further demonstrated GSK3 as a key driver of the memory deficits in male Tg26 mice. We showed increased hippocampal GSK3 activity in male Tg26 mice compared to male WT mice. Excitingly, when male Tg26 mice were treated with a selective GSK3 inhibitor, TDZD-8, we observed a significant increase in hippocampal phospho-Ser831 GluA1, synapsin-1 and BDNF protein levels as well as a complete restoration of hippocampal synaptic transmission, LT, and contextual fear memory. In accordance with our findings, hyperactivity of GSK3 has been reported to induce impairments in novel object recognition (Pardo, Abrial, Jope, & Beurel, 2016). Additionally, inhibition of GSK3 was shown to increase synapsin-1 expression and promote synaptogenesis in cultured neurons, increase hippocampal BDNF expression, increase GluA1 membrane levels and facilitate LTP (Beurel, Grieco, Amadei, Downey, & Jope, 2016; Cuesto et al., 2015; Fukumoto, Morinobu, Okamoto, Kagaya, & Yamawaki, 2001; Hooper et al., 2007). In this study, TDZD-8 treatment in male Tg26 mice did not alter hippocampal HIV-1 LTR mRNA expression, although previous studies have reported GSK3 inhibition to suppress HIV-1 replication (Guendel et al., 2014; Kehn-Hall et al., 2011). Nonetheless, since GSK3 inhibition also protects against HIV-induced neurotoxicity (Everall et al., 2002; Maggirwar, Tong, Ramirez, Gelbard, & Dewhurst, 1999; Masvekar, El-Hage, Hauser, & Knapp, 2015), our findings strongly suggest that selective inhibition of GSK3 with blood-brain-barrier permeable drugs such as TDZD-8 may have excellent therapeutic benefit in HAND.

Lack of a suitable animal model that mimics human conditions is one of the major limitations in developing adjunctive therapies for HAND. The Tg26 mouse, which expresses replication-deficient proviral genes, allowed us to study the effects of chronic stress from multiple HIV-1 viral proteins on cognition and is therefore a clinically relevant model that recapitulates, at least partly, HIV-1 patients on antiretroviral therapy. In addition, being a non-infectious mouse makes it highly suitable for behavioural studies. Limitations of this model however include lack of infectious processes of HIV-1, expression of proviral genes in all cell types and tissues, lack of complete

viral genome and development of immune tolerance to HIV-1 transgene products. The aforementioned limitations of this mouse model warrant further investigation on the effects of TDZD-8 on learning and memory in other models of HIV-1. In addition, it remains to be determined whether development of cognitive deficits in older female Tg26 mice (Putatunda et al., 2019) is regulated by increased GSK3 activity. Furthermore, in this study, we investigated only the short-term effects of TDZD-8 (24-h treatment) on contextual fear memory and synaptic impairments in male Tg26 mice. Future studies will determine the effects of long-term treatment with TDZD-8 on spatial learning and memory and hippocampal neurogenesis in Tg26 mice (Putatunda et al., 2018), given that GSK3 inhibition improves spatial learning and promotes neurogenesis both in vitro and in vivo (Franklin et al., 2014; Morales-Garcia et al., 2012).

In conclusion, our results effectively demonstrate that neurocognitive deficits in Tg26 mice are sex-dependent, stressing the importance of incorporating sex as a biological variable in studies of HAND. Furthermore, we provide evidence that GSK3 inhibition rescues hippocampal-associated synaptic and memory impairments in Tg26 mice. While several of the existing therapeutic strategies for HAND have failed or have had only limited beneficial outcome (McGuire, Barrett, Vezina, Spitsin, & Douglas, 2014), GSK3 inhibitors with CNS bioavailability such as TDZD-8 (Franklin et al., 2014; Martinez, Alonso, Castro, Perez, & Moreno, 2002; Xie et al., 2016) may emerge as a promising new adjunctive therapy to improve episodic memory in people living with HIV-1.

ACKNOWLEDGEMENTS

We thank Dr. Roy Lee Sutliff (Emory University School of Medicine, Atlanta, GA) for kindly providing us with Tg26 mice breeders. We also thank Giselle Rodriguez and Irina Chupikova for the help with genotyping and Dr. Katherina Walz and Dr. Clemer Abad (Mouse Behavior Core, University of Miami) for their technical support and advise. This study was supported by the National Institutes of Health Grants R01 DA043252, R01 DA044582, R01 DA047089 and R01 DA050542 awarded to S.R. and by the Miami Center for AIDS Research (CFAR) via a pilot grant (P30AI073961) awarded to S.M. The CFAR programme at the NIH includes the following co-funding and participating institutes and centres: NIAID, NCI, NICHD, NHLBI, NIDA, NIMHD, NIA, NIDDK, NIDCR, NIMH, NINR, NIGMS and OD.

AUTHOR CONTRIBUTIONS

S.M., M.A.B., E.B., C.M.A. and S.R. designed the project. S.M. conceptualized and designed the experiments, bred mice and performed the mouse genotyping, genomic DNA, qRT-PCR, western blot and ELISA experiments, microscopy and analysis. S.M. and M.A.B. designed and performed behavioural studies and data analysis. D.J.T. performed electrophysiology experiments and analysis. E.B. guided the experiments with TDZD-8. J.M. performed immunohistochemistry and H&E staining. U.K. performed qRT-PCR and analysed IHC data. R.J. assisted in the tissue collection and processing. S.M. wrote the first draft of the manuscript. M.A.B., D.J.T., E.B., S.R., C.M.A. and S.R. edited previous versions of the manuscript.

CONFLICT OF INTEREST

All authors declare no competing financial interests. S.R. and S.M. have a pending U.S. patent (Application number: 62/879,212) related to this work.

DECLARATION OF TRANSPARENCY AND SCIENTIFIC RIGOUR

This Declaration acknowledges that this paper adheres to the principles for transparent reporting and scientific rigour of preclinical research as stated in the *BJP* guidelines for [Design & Analysis](#), [Immunoblotting and Immunochemistry](#) and [Animal Experimentation](#) and as recommended by funding agencies, publishers and other organizations engaged with supporting research.

DATA AVAILABILITY STATEMENT

The data that support the findings of this study are available from the corresponding author upon reasonable request. Some data may not be made available because of privacy or ethical restrictions.

ORCID

Shamsudheen Moidunny  <https://orcid.org/0000-0002-2499-0788>

REFERENCES

- Abràmoff, M. D., Magalhães, P. J., & Ram, S. J. (2004). Image processing with imageJ. *Laurin Publishing, Biophotonics International*, 11(7), 36–42.
- Alexander, S., Roberts, R. E., Broughton, B., Sobey, C. G., George, C. H., Stanford, S. C., ... Ahluwalia, A. (2018). Goals and practicalities of immunoblotting and immunohistochemistry: A guide for submission to the *British Journal of Pharmacology*. *British Journal of Pharmacology*, 175(3), 407–411. <https://doi.org/10.1111/bph.14112>
- Alexander, S. P. H., Fabbro, D., Kelly, E., Mathie, A., Peters, J. A., Veale, E. L., ... CGTP Collaborators. (2019). The concise guide to pharmacology 2019/20: Enzymes. *British Journal of Pharmacology*, 176, S297–S396. <https://doi.org/10.1111/bph.14752>
- Bachis, A., Avdoshina, V., Zecca, L., Parsadianian, M., & Mocchetti, I. (2012). Human immunodeficiency virus type 1 alters brain-derived neurotrophic factor processing in neurons. *The Journal of Neuroscience*, 32, 9477–9484. <https://doi.org/10.1523/JNEUROSCI.0865-12.2012>
- Beurel, E., Grieco, S. F., Amadei, C., Downey, K., & Jope, R. S. (2016). Ketamine-induced inhibition of glycogen synthase kinase-3 contributes to the augmentation of α -amino-3-hydroxy-5-methylisoxazole-4-propionic acid (AMPA) receptor signaling. *Bipolar Disorders*, 18, 473–480. <https://doi.org/10.1111/bdi.12436>
- Chow, F. C., Regan, S., Zanni, M. V., Looby, S. E., Bushnell, C. D., Meigs, J. B., ... Triant, V. A. (2018). Elevated ischemic stroke risk among women living with HIV infection. *Aids*, 32(1), 59–67. <https://doi.org/10.1097/QAD.0000000000001650>
- Cuesto, G., Jordán-Álvarez, S., Enriquez-Barreto, L., Ferrus, A., Morales, M., & Acebes, A. (2015). GSK3 β inhibition promotes synaptogenesis in *Drosophila* and mammalian neurons. *PLoS ONE*, 10(3), e0118475. <https://doi.org/10.1371/journal.pone.0118475>
- Curtis, M. J., Alexander, S., Cirino, G., Docherty, J. R., George, C. H., Giembycz, M. A., ... Ahluwalia, A. (2018). Experimental design and analysis and their reporting II: Updated and simplified guidance for authors and peer reviewers. *British Journal of Pharmacology*, 175(7), 987–993. <https://doi.org/10.1111/bph.14153>
- Das, B., Dobrowolski, C., Luttge, B., Valadkhan, S., Chomont, N., Johnston, R., ... Karn, J. (2018). Estrogen receptor-1 is a key regulator of HIV-1 latency that imparts gender-specific restrictions on the latent reservoir. *Proceedings of the National Academy of Sciences*, 115(33), E7795–E7804. <https://doi.org/10.1073/pnas.1803468115>
- Dickie, P., Felser, J., Eckhaus, M., Bryant, J., Silver, J., Marinos, N., & Notkins, A. L. (1991). HIV-associated nephropathy in transgenic mice expressing HIV-1 genes. *Virology*, 185(1), 109–119. [https://doi.org/10.1016/0042-6822\(91\)90759-5](https://doi.org/10.1016/0042-6822(91)90759-5)
- Divani, A. A., Murphy, A. J., Meints, J., Sadeghi-Bazargani, H., Nordberg, J., Monga, M., ... SantaCruz, K. S. (2015). A novel preclinical model of moderate primary blast-induced traumatic brain injury. *Journal of Neurotrauma*, 32(14), 1109–1116. <https://doi.org/10.1089/neu.2014.3686>
- Everall, I. P., Bell, C., Mallory, M., Langford, D., Adame, A., Rockenstein, E., & Masliah, E. (2002). Lithium ameliorates HIV-gp120-mediated neurotoxicity. *Molecular and Cellular Neurosciences*, 21(3), 493–501. <https://doi.org/10.1006/mcne.2002.1196>
- Faílde-Garrido, J. M., Alvarez, M. R., & Simón-López, M. A. (2008). Neuropsychological impairment and gender differences in HIV-1 infection. *Psychiatry and Clinical Neurosciences*, 62(5), 494–502. <https://doi.org/10.1111/j.1440-1819.2008.01841.x>
- Fields, J., Dumaop, W., Langford, T. D., Rockenstein, E., & Masliah, E. (2014). Role of neurotrophic factor alterations in the neurodegenerative process in HIV associated neurocognitive disorders. *Journal of Neuroimmune Pharmacology*, 9, 102–116. <https://doi.org/10.1007/s11481-013-9520-2>
- Fischer, A. H., Jacobson, K. A., Rose, J., & Zeller, R. (2008). Hematoxylin and eosin staining of tissue and cell sections. *CSH Protocols*, 2008, pdb.prot4986. <https://doi.org/10.1101/pdb.prot4986>
- Fitting, S., Ignatowska-Jankowska, B. M., Bull, C., Skoff, R. P., Lichtman, A. H., Wise, L. E., ... Hauser, K. F. (2013). Synaptic dysfunction in the hippocampus accompanies learning and memory deficits in human immunodeficiency virus type-1 Tat transgenic mice. *Biological Psychiatry*, 73(5), 443–453. <https://doi.org/10.1016/j.biopsych.2012.09.026>
- Fogel, J., Rubin, L. H., Maki, P., Keutmann, M. K., Gonzalez, R., Vassileva, J., & Martin, E. M. (2017). Effects of sex and HIV serostatus on spatial navigational learning and memory among cocaine users. *Journal of Neurovirology*, 23(6), 855–863. <https://doi.org/10.1007/s13365-017-0563-7>
- Franklin, A. V., King, M. K., Palomo, V., Martinez, A., McMahon, L. L., & Jope, R. S. (2014). Glycogen synthase kinase-3 inhibitors reverse deficits in long-term potentiation and cognition in fragile X mice. *Biological Psychiatry*, 75(3), 198–206. <https://doi.org/10.1016/j.biopsych.2013.08.003>
- Fukumoto, T., Morinobu, S., Okamoto, Y., Kagaya, A., & Yamawaki, S. (2001). Chronic lithium treatment increases the expression of brain-derived neurotrophic factor in the rat brain. *Psychopharmacology*, 158(1), 100–106. <https://doi.org/10.1007/s002130100871>
- Gelman, B. B., & Nguyen, T. P. (2010). Synaptic proteins linked to HIV-1 infection and immunoproteasome induction: Proteomic analysis of human synaptosomes. *Journal of Neuroimmune Pharmacology*, 5, 92–102. <https://doi.org/10.1007/s11481-009-9168-0>
- Goodkin, K., Miller, E. N., Cox, C., Reynolds, S., Becker, J. T., Martin, E., ... Sacktor, N. C. (2017). Effect of ageing on neurocognitive function by stage of HIV infection: Evidence from the Multi-Center AIDS Cohort Study. *Lancet HIV*, 4(9), e411–e422. [https://doi.org/10.1016/S2352-3018\(17\)30098-X](https://doi.org/10.1016/S2352-3018(17)30098-X)
- Guendel, I., Iordanskiy, S., Van Duyne, R., Kehn-Hall, K., Saifuddin, M., Das, R., ... Kashanchi, F. (2014). Novel neuroprotective GSK-3 β inhibitor restricts Tat-mediated HIV-1 replication. *Journal of Virology*, 88(2), 1189–1208. <https://doi.org/10.1128/JVI.01940-13>
- Hahn, Y. K., Podhaizer, E. M., Farris, S. P., Miles, M. F., Hauser, K. F., & Knapp, P. E. (2015). Effects of chronic HIV-1 Tat exposure in the CNS: Heightened vulnerability of males versus females to changes in cell numbers, synaptic integrity, and behavior. *Brain Structure &*

- Function, 220(2), 605–623. <https://doi.org/10.1007/s00429-013-0676-6>
- Hooper, C., Markevich, V., Plattner, F., Killick, R., Schofield, E., Engel, T., ... Lovestone, S. (2007). Glycogen synthase kinase-3 inhibition is integral to long-term potentiation. *The European Journal of Neuroscience*, 25(1), 81–86. <https://doi.org/10.1111/j.1460-9568.2006.05245.x>
- Jovanovic, J. N., Czernik, A. J., Fienberg, A. A., Greengard, P., & Sihra, T. S. (2000). Synapsins as mediators of BDNF-enhanced neurotransmitter release. *Nature Neuroscience*, 3, 323–329. <https://doi.org/10.1038/73888>
- Kehn-Hall, K., Guendel, I., Carpio, L., Skaltsounis, L., Meijer, L., Al-Harhi, L., ... Kashanchi, F. (2011). Inhibition of Tat-mediated HIV-1 replication and neurotoxicity by novel GSK3- β inhibitors. *Virology*, 415(1), 56–68. <https://doi.org/10.1016/j.virol.2011.03.025>
- Kelschenbach, J., He, H., Kim, B. H., Borjabad, A., Gu, C. J., Chao, W., ... Volsky, D. J. (2019). Efficient expression of HIV in immunocompetent mouse brain reveals a novel nonneurotoxic viral function in hippocampal synaptodendritic injury and memory impairment. *MBio*, 10(4), e00591–e00519. <https://doi.org/10.1128/mBio.00591-19>
- Keutmann, M. K., Gonzalez, R., Maki, P. M., Rubin, L. H., Vassileva, J., & Martin, E. M. (2017). Sex differences in HIV effects on visual memory among substance-dependent individuals. *Journal of Clinical and Experimental Neuropsychology*, 39(6), 574–586. <https://doi.org/10.1080/13803395.2016.1250869>
- King, M. K., Pardo, M., Cheng, Y., Downey, K., Jope, R. S., & Beurel, E. (2014). Glycogen synthase kinase-3 inhibitors: Rescuers of cognitive impairments. *Pharmacology & Therapeutics*, 141(1), 1–12. <https://doi.org/10.1016/j.pharmthera.2013.07.010>
- Leal, G., Comprido, D., & Duarte, C. B. (2014). BDNF-induced local protein synthesis and synaptic plasticity. *Neuropharmacology*, 76, 639–656. <https://doi.org/10.1016/j.neuropharm.2013.04.005>
- Lilley, E., Stanford, S.C., Kendall, D.E., Alexander, S.P., Cirino, G., Docherty, J.R., George, C.H., Insel, P.A., Izzo, A.A., Ji, Y., Panettieri, R. A., Sobey, C.G., Stefanska, B., Stephens, G., Teixeira, M., & Ahluwalia, A. (2020). ARRIVE 2.0 and the *British Journal of Pharmacology*: Updated guidance for 2020. *British Journal of Pharmacology*, 177(16), 3611–3616. <https://doi.org/10.1111/bph.15178>
- Livak, K. J., & Schmittgen, T. D. (2001). Analysis of relative gene expression data using real-time quantitative PCR and the $2^{-\Delta\Delta CT}$ method. *Methods*, 25(4), 402–408. <https://doi.org/10.1006/meth.2001.1262>
- Luine, V., & Frankfurt, M. (2013). Interactions between estradiol, BDNF and dendritic spines in promoting memory. *Neuroscience*, 239, 34–45. <https://doi.org/10.1016/j.neuroscience.2012.10.019>
- Maggirwar, S. B., Tong, N., Ramirez, S., Gelbard, H. A., & Dewhurst, S. (1999). HIV-1 Tat-mediated activation of glycogen synthase kinase-3 β contributes to Tat-mediated neurotoxicity. *Journal of Neurochemistry*, 73, 578–586. <https://doi.org/10.1046/j.1471-4159.1999.0730578.x>
- Maren, S., Phan, K. L., & Liberzon, I. (2013). The contextual brain: Implications for fear conditioning, extinction and psychopathology. *Nature Reviews Neuroscience*, 14(6), 417–428. <https://doi.org/10.1038/nrn3492>
- Martinez, A., Alonso, M., Castro, A., Perez, C., & Moreno, F. J. (2002). First non-ATP competitive glycogen synthase kinase 3 β (GSK-3 β) inhibitors: Thiadiazolidinones (TDZD) as potential drugs for the treatment of Alzheimer's disease. *Journal of Medicinal Chemistry*, 45(6), 1292–1299. <https://doi.org/10.1021/jm011020u>
- Martin-Fernandez, M., Jamison, S., Robin, L. M., Zhao, Z., Martin, E. D., Aguilar, J., ... Araque, A. (2017). Synapse-specific astrocyte gating of amygdala-related behavior. *Nature Neuroscience*, 20(11), 1540–1548. <https://doi.org/10.1038/nn.4649>
- Masvekar, R. R., El-Hage, N., Hauser, K. F., & Knapp, P. E. (2015). GSK3 β activation is a point of convergence for HIV-1 and opiate-mediated interactive neurotoxicity. *Molecular and Cellular Neurosciences*, 65, 11–20. <https://doi.org/10.1016/j.mcn.2015.01.001>
- McGuire, J. L., Barrett, J. S., Vezina, H. E., Spitsin, S., & Douglas, S. D. (2014). Adjuvant therapies for HIV-associated neurocognitive disorders. *Annals of Clinical Translational Neurology*, 1(11), 938–952. <https://doi.org/10.1002/acn3.131>
- McGuire, J. L., Gill, A. J., Douglas, S. D., Kolson, D. L., & CNS HIV anti-retroviral therapy effects research (CHARTER) group. (2015). Central and peripheral markers of neurodegeneration and monocyte activation in HIV-associated neurocognitive disorders. *Journal of Neurovirology*, 21(4), 439–448. <https://doi.org/10.1007/s13365-015-0333-3>
- McLaurin, K. A., Booze, R. M., & Mactutus, C. F. (2018). Evolution of the HIV-1 transgenic rat: Utility in assessing the progression of HIV-1-associated neurocognitive disorders. *Journal of Neurovirology*, 24(2), 229–245. <https://doi.org/10.1007/s13365-017-0544-x>
- McLaurin, K. A., Booze, R. M., Mactutus, C. F., & Fairchild, A. J. (2017). Sex matters: Robust sex differences in signal detection in the HIV-1 transgenic rat. *Frontiers in Behavioral Neuroscience*, 11, 212. <https://doi.org/10.3389/fnbeh.2017.00212>
- McLaurin, K. A., Li, H., Booze, R. M., & Mactutus, C. F. (2019). Disruption of timing: NeuroHIV progression in the Post-cART era. *Scientific Reports*, 9(1), 827. <https://doi.org/10.1038/s41598-018-36822-1>
- Moidunny, S., Matos, M., Wesseling, E., Banerjee, S., Volsky, D. J., Cunha, R. A., ... Roy, S. (2016). Oncostatin M promotes excitotoxicity by inhibiting glutamate uptake in astrocytes: Implications in HIV-associated neurotoxicity. *Journal of Neuroinflammation*, 13(1), 144. <https://doi.org/10.1186/s12974-016-0613-8>
- Morales-García, J. A., Luna-Medina, R., Alonso-Gil, S., Sanz-Sancristobal, M., Palomo, V., Gil, C., & Perez-Castillo, A. (2012). Glycogen synthase kinase 3 inhibition promotes adult hippocampal neurogenesis in vitro and in vivo. *ACS Chemical Neuroscience*, 3(11), 963–971. <https://doi.org/10.1021/cn300110c>
- Nielsen, D. M., & Cnric, L. S. (2002). Automated analysis of foot-shock sensitivity and concurrent freezing behavior in mice. *Journal of Neuroscience Methods*, 115(2), 199–209. [https://doi.org/10.1016/s0165-0270\(02\)00020-1](https://doi.org/10.1016/s0165-0270(02)00020-1)
- Pandey, G. N., Dwivedi, Y., Rizavi, H. S., Teppen, T., Gaszner, G. L., Roberts, R. C., & Conley, R. R. (2009). GSK-3 β gene expression in human postmortem brain: Regional distribution, effects of age and suicide. *Neurochemical Research*, 34(2), 274–285. <https://doi.org/10.1007/s11064-008-9770-1>
- Pardo, M., Abrial, E., Jope, R. S., & Beurel, E. (2016). GSK3 β isoform-selective regulation of depression, memory and hippocampal cell proliferation. *Genes Brain Behavior*, 15(3), 348–355. <https://doi.org/10.1111/gbb.12283>
- Percie du Serf N., Hurst V., Ahluwalia A., Alam S., Avey M.T., Baker M., Browne W.J., Clark A., Cuthill I.C., Dirnagl U., Emerson M., Garner P., Holgate S.T., Howells D.W., Karp N.A., Lazic S.E., Lidster K., MacCallum C.J., Macleod M., Pearl E.J., Petersen O., Rawle F., Reynolds P., Rooney K., Sena E.S., Silberberg S.D., Steckler T., & Würbel H. (2020). The ARRIVE guidelines 2.0: Updated guidelines for reporting animal research. *PLoS Biology*, 18(7), e3000410. <https://doi.org/10.1371/journal.pbio.3000410>
- Putatunda, R., Zhang, Y., Li, F., Fagan, P. R., Zhao, H., Ramirez, S. H., ... Hu, W. (2019). Sex-specific neurogenic deficits and neurocognitive disorders in middle-aged HIV-1 Tg26 transgenic mice. *Brain, Behavior, and Immunity*, 80, 488–499. <https://doi.org/10.1016/j.bbi.2019.04.029>
- Putatunda, R., Zhang, Y., Li, F., Yang, X. F., Barbe, M. F., & Hu, W. (2018). Adult neurogenic deficits in HIV-1 Tg26 transgenic mice. *Journal of Neuroinflammation*, 15(1), 287. <https://doi.org/10.1186/s12974-018-1322-2>
- Robertson, K., Bayon, C., Molina, J. M., McNamara, P., Resch, C., Munoz-Moreno, J. A., ... Wyk, J. V. (2014). Screening for neurocognitive impairment, depression, and anxiety in HIV-infected patients in Western Europe and Canada. *AIDS Care*, 26(12), 1555–1561. <https://doi.org/10.1080/09540121.2014.936813>

- Rogers, D. C., Fisher, E. M. C., Brown, S. D. M., Peters, J., Hunter, A. J., & Martin, J. E. (1997). Behavioral and functional analysis of mouse phenotype: SHIRPA, a proposed protocol for comprehensive phenotype assessment. *Mammalian Genome*, 8, 711–713. <https://doi.org/10.1007/s003359900551>
- Saylor, D., Dickens, A. M., Sacktor, N., Haughey, N., Slusher, B., Pletnikov, M., ... McArthur, J. C. (2016). HIV-associated neurocognitive disorder—Pathogenesis and prospects for treatment. *Nature Reviews. Neurology*, 12(4), 234–248. <https://doi.org/10.1038/nrneuro.2016.27>
- Sutherland, C., Leighton, I. A., & Cohen, P. (1993). Inactivation of glycogen synthase kinase-3 β by phosphorylation: New kinase connections in insulin and growth-factor signalling. *The Biochemical Journal*, 296, 15–19. <https://doi.org/10.1042/bj2960015>
- Titus, D. J., Wilson, N. M., Freund, J. E., Carballosa, M. M., Sikah, K. E., Furones, C., ... Atkins, C. M. (2016). Chronic cognitive dysfunction after traumatic brain injury is improved with a phosphodiesterase 4B inhibitor. *The Journal of Neuroscience*, 36(27), 7095–7108. <https://doi.org/10.1523/JNEUROSCI.3212-15.2016>
- Valcour, V., Shikuma, C., Shiramizu, B., Watters, M., Poff, P., Selnes, O., ... Sacktor, N. (2004). Higher frequency of dementia in older HIV-1 individuals: The Hawaii aging with HIV-1 cohort. *Neurology*, 63(5), 822–827. <https://doi.org/10.1212/01.wnl.0000134665.58343.8d>
- Wisniewski, A. B., Apel, S., Selnes, O. A., Nath, A., McArthur, J. C., & Dobs, A. S. (2005). Depressive symptoms, quality of life, and neuropsychological performance in HIV/AIDS: The impact of gender and injection drug use. *Journal of Neurovirology*, 11(2), 138–143. <https://doi.org/10.1080/13550280590922748>
- Woodgett, J. R. (1990). Molecular cloning and expression of glycogen synthase kinase-3/factor A. *The EMBO Journal*, 9(8), 2431–2438.
- Xie, C. L., Lin, J. Y., Wang, M. H., Zhang, Y., Zhang, S. F., Wang, X. J., & Liu, Z. G. (2016). Inhibition of glycogen synthase kinase-3 β (GSK-3 β) as potent therapeutic strategy to ameliorate L-DOPA-induced dyskinesia in 6-OHDA Parkinsonian rats. *Scientific Reports*, 6, 23527. <https://doi.org/10.1038/srep23527>
- Zhu, L. Q., Wang, S. H., Liu, D., Yin, Y. Y., Tian, Q., Wang, X. C., ... Wang, J. Z. (2007). Activation of glycogen synthase kinase-3 inhibits long-term potentiation with synapse-associated impairments. *The Journal of Neuroscience*, 27(45), 12211–12220. <https://doi.org/10.1523/JNEUROSCI.3321-07.2007>

SUPPORTING INFORMATION

Additional supporting information may be found online in the Supporting Information section at the end of this article.

How to cite this article: Moidunny S, Benneyworth MA, Titus DJ, et al. Glycogen synthase kinase-3 inhibition rescues sex-dependent contextual fear memory deficit in human immunodeficiency virus-1 transgenic mice. *Br J Pharmacol*. 2020;177:5658–5676. <https://doi.org/10.1111/bph.15288>